

AMERICAN UNIVERSITY OF BEIRUT

EFFECT OF FRACTURE NETWORK COMPLEXITY AND  
EVOLUTION ON FRACTURING FLUID RECOVERY AND  
ITS IMPLICATIONS ON AQUIFERS' SAFETY

by  
SARA HUSSEIN MAKKI

A thesis  
submitted in partial fulfillment of the requirements  
for the degree of Master of Engineering  
to the Baha and Walid Bassatne Department of Chemical Engineering  
and Advanced Energy  
of the Maroun Semaan Faculty of Engineering and Architecture  
at the American University of Beirut

Beirut, Lebanon  
August 2022

AMERICAN UNIVERSITY OF BEIRUT

EFFECT OF FRACTURE NETWORK COMPLEXITY AND  
EVOLUTION ON FRACTURING FLUID RECOVERY AND  
ITS IMPLICATIONS ON AQUIFERS' SAFETY

by  
SARA HUSSEIN MAKKI

Approved by:

Signature

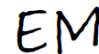


---

Dr. Alissar Yehya, Assistant Professor  
Department of Civil and Environmental Engineering

Advisor

Signature



---

Dr. Elsa Maalouf, Assistant Professor  
Department of Chemical Engineering and Advanced Energy

Co-Advisor

Signature



---

Dr. Tony Nemer, Assistant Professor  
Department of Geology

Member of Committee

Signature



---

Dr. Kassem Ghorayeb, Assistant Professor  
Department of Chemical Engineering and Advanced Energy

Member of Committee

Date of thesis defense: August 30, 2022



## ACKNOWLEDGEMENTS

First of all, all thanks go to God for His blessings and for giving me the strength to complete this research.

I would like to convey my deepest gratitude to my advisors, Dr. Alissar Yehya and Dr. Elsa Maalouf, for providing me with the opportunity to join their research group and work under their supervision. Their knowledge, guidance, and support were crucial to the success of this research. I would also like to appreciate their continuous cooperation and patience.

A special thanks to Dr. Kassem Ghorayeb and Dr. Tony Nemer for being on my thesis committee.

Last but not least, I would like to acknowledge the support and motivation my family and friends provided me with throughout this journey.

# ABSTRACT

## OF THE THESIS OF

Sara Hussein Makki

for

Master of Engineering

Major: Chemical Engineering

Title: Effect of Fracture Network Complexity and Evolution on Fracturing Fluid Recovery and its Implications on Aquifers' Safety

It has been reported that the recovery of the fluid injected during hydraulic fracturing (HF) is considerably low. Hence, the fate of the fracturing fluid in the subsurface and its migration become a concern for water aquifers contamination. In this work, we study the migration of fracturing fluid and track its distribution in fractured reservoirs using a two-dimensional finite element model with multi-phase and multi-component flow. We determine the effect of fracture network complexity (represented by interconnecting hydraulic conduits or faults), HF shut-in period, formation and fault permeability and its temporal evolution - driven by pressure changes - on fracturing fluid recovery. Our results indicate that extending the shut-in period curbs the recovery and increasing network complexity results in a larger fluid loss into the formation. Moreover, we found that the correlation between the subsurface permeability structure and the recovery is not straightforward; the recovery increases when the permeability of faults increases and decreases when the permeability of the layers surrounding the HF zone increases. Our findings also show that the pressure-dependency of the permeability, i.e., fractures and cracks open during high pressure injection and close or partially close when the pressure is released, significantly affects the flow-back recovery. This can further justify the observed low fluid recovery rates in most cases. Finally, we show that the time needed for trapped fracking fluid to migrate to nearby aquifers ranges from a few months to hundreds of years. Consequently, it is crucial to assess the long-term effects of the hydraulic fracturing practices since the associated environmental hazards might require several years to be noticed or detected.

# TABLE OF CONTENTS

ACKNOWLEDGEMENTS .....	1
ABSTRACT .....	2
ILLUSTRATIONS .....	5
TABLES.....	7
INTRODUCTION.....	8
LITERATURE REVIEW.....	15
2.1 Environmental Impact of Fracturing Fluids.....	15
2.1.1 Fracturing Fluid Composition .....	15
2.1.2 Associated Risks .....	16
2.2 The Fate of the Fracturing Fluid .....	21
2.2.1 Parameters Affecting Flowback.....	21
2.2.2 Effect of Fracture Network Complexity on Load Recovery and Oil/Gas Production.....	26
2.2.3 Seismicity Induced by Fluid Diffusion .....	31
METHODOLOGY .....	39
3.1 Model Description .....	39
3.2 Modeling Scenarios .....	43
3.3 Theory .....	44
3.3.1 Mathematical Model .....	44
3.3.2 Initial and Boundary Conditions .....	46
3.3.3 Pressure-dependent Permeability .....	47

3.3.4 Recovery Calculation .....	49
<b>RESULTS AND DISCUSSION .....</b>	<b>50</b>
4.1 Base case scenarios .....	51
4.2 Parametric study .....	51
4.2.1 Effect of shut-in and injection periods .....	52
4.2.2 Effect of subsurface permeability structure .....	55
4.2.3 Effect of temporal evolution of permeability .....	59
4.3 Discussion .....	62
4.3.1 Limitations .....	62
4.3.2 Implications on the safety of nearby aquifers .....	63
<b>CONCLUSION .....</b>	<b>66</b>
<b>APPENDIX .....</b>	<b>68</b>
<b>REFERENCES .....</b>	<b>69</b>

# ILLUSTRATIONS

Figure

1. Water Based Fracturing Fluid Composition (reproduced from Shah et al., 2015) .....	15
2. Toxicity Information for the 194 Fracturing Fluid Constituents with Accessible Data Out of the 925 Constituents Studied (Elliot et al., 2016) .....	19
3. Percentage of Chemicals Associated with (a) Reproductive Toxicity, and (b) Developmental Toxicity, Based on the Number of Chemicals with Available Toxicity Data (Elliot et al., 2016) .....	20
4. Load Recovery vs Shut-in Periods in Several Studies .....	23
5. The Speed of Fluid's Upward Migration as a Function of Increase in Different Parameters Studied in the Literature ( Gassiat et al., 2013; Pfunt et al., 2016; Taherdangkoo et al., 2017; Taherdangkoo et al., 2019).....	24
6. The Effect of Increase in Different Parameters Studied in the Literature on Water Leak-off ( Ghaderi et al., 2018; Li et al., 2007; McClure, 2014; Wang et al., 2017; Yang et al., 2015) .....	26
7. Schematic of the 2D Model Showing the Permeability of the Layers and of the Hydraulic Conduit and the Four Horizontal Wells with Spacing of 600 m (Figure Not to Scale).....	40
8. Schematic Description of (a) Scenario 1 (SC1), (b) Scenario 2 (SC 2), (c) Scenario 3 (SC3), and (d) Scenario 4 .....	44
9. Pressure-dependent Permeability During Shut-in and Production of the (a) Hydraulic Fracturing Zone, and (b) Fault Zone .....	48
10. Locations of Points A-H.....	50
11. Recovery Values for the Base Case Scenarios .....	51
12. Recovery Values for Different Shut-in and Injection Periods .....	54
13. Normalized Concentration Change vs. Flow-Back Time for 5 and 30 Days of Shut-In Period Measured (a) at Point A in SC1, (b) at Point B in SC2, (b) at Point C in SC3, and (d) at Point D in SC4. Points A-D are Shown in Figure 1055	55
14. Recovery Values for the Base Case and for Increased Permeability of Layers 1 and 2 .....	56
15. Recovery Values for the Base Case and for Increased Permeability of Faults 2 and 3 .....	56

16. Total Flux vs. Flow-back Time Measured (a) at Point E in SC3 for Different Permeability Values of Fault 2, and (b) at Points F and G in SC4 for Different Permeability Values of Fault 3. Figure 10 Shows the Locations of Points E, F, and G .....	59
17. Permeability of the HF Region, Fault 1, Fault 2, and Fault 3 as a Function of Post Injection Time for SC4 when Assuming a Pressure -dependent Permeability Model.....	60
18. Recovery Values for the Base Case Scenarios and the Formation with Pressure-dependent Permeability .....	61
19. Normalized Concentration Change in SC4 at Point H (Shown in Figure 10) vs Flow-back Time for a Formation with Constant Permeability and a Pressure-dependent Permeability .....	62
20. Time Needed for the Fluid to Migrate vs. the Distance Between the Fluid and the Aquifer for Different Values of Net Driving Pressure Per Linear Meter and for Permeability (a) $k_{avg}$ , and (b) $100k_{avg}$ .....	65

## TABLES

### Table

21. Drinking Water Contamination Incidents Linked to Hydraulic Fracturing Operations in the United States (Birdsell et al., 2015).....	17
22. The Correlation Between Different Parameters Studied in the Literature and the Load Recovery .....	22
23. The Stages of the Simulation .....	39
24. Parameters Used in the Simulation .....	42
25. Description of the Scenarios .....	43
26. Load Recovery Values Resulting from the Parametric Study .....	52
27. Permeability Values of Layers 1 &2, Fault 2, and Fault 3 for Different Cases ..	57

# CHAPTER 1

## INTRODUCTION

The growth in shale exploitation has been driven, throughout the years, by the combined improvements in directional drilling and multistage hydraulic fracturing technologies (Fu & Dehghanpour, 2020; Jia et al., 2013; McClure, 2014; Osborn et al., 2011; Vidic et al., 2013) that are required to effectively deplete the hydrocarbon-rich shale formations with extremely low permeability values (Kissinger et al., 2013; Liu et al., 2019; Reagan et al., 2015; Veatch, 1983; Wang et al., 2017). Fracking consists of injecting large volumes of fracturing fluid at high pressures into the subsurface to initiate new fractures and re-activate pre-existing fractures, which creates a high-permeability conduit between the target reservoir and the producing well (Abaa et al., 2013; Gassiat et al., 2013; King, 2012; Osselin et al., 2018; Sarkar et al., 2016; Seales et al., 2017). Disparities in the flow-back recovery of fracturing fluid are reported in the industry, with values ranging between 5% and 50% during the first months of production (Birkle, 2016; Fan et al., 2010; Henderson et al., 2011; King, 2012; Osselin et al., 2018; Robart, 2012; Zhou et al., 2016). For instance, Osselin et al. (2018) estimated a 36% fracking fluid recovery from a horizontal well in the low-permeability Montney formation reservoir in Alberta, Canada by using chemical tracer and flow-back field data. Furthermore, a 9.6% recovery was quantified by Birkle (2016) using geochemical fingerprinting of samples collected from a well in Qusaiba shale in Saudi Arabia.

Inspecting the disparity in recovery values, while keeping in mind the large volumes of fluid employed in the process (Jia et al., 2013; McClure, 2014), raises questions about one of the most alarming aspects of hydraulic fracturing, which is the fate of the fracturing fluid. This issue has become an environmental concern because the most common fracturing fluid is slick-water (Liao et al., 2019) that is composed mainly of freshwater with a small percentage of additives like guar gum, petroleum distillates, surfactants, corrosion inhibitors, and friction reducers in addition to the propping material (Arthur et al., 2008; Henderson et al., 2011). These additives cause serious drinking water contamination if the HF fluid migrates upwards from the shale, through conduit structures or formations, towards shallow aquifers (Birdsell et al., 2015; Gassiat et al., 2013; Kissinger et al., 2013; Lange et al., 2013; Llewellyn et al., 2015; Myers, 2012; Taherdangkoo et al., 2019).

Although modeling results suggest that the probability of fracturing fluid reaching aquifers is low (Arthur et al., 2008; Birdsell et al., 2015; Gassiat et al., 2013; Kissinger et al., 2013; Myers, 2012; Osborn et al., 2011; Pfunter et al., 2016; Taherdangkoo et al., 2019; Taherdangkoo et al., 2017), there are reported cases of traces of methane and fracturing fluid detected in water wells (Llewellyn et al., 2015; Osborn et al., 2011). Furthermore, methane detection suggests that the same pathway that allowed the migration of gas can serve as a pathway for fracturing fluid migration (Gassiat et al., 2013; Myers, 2012). Moreover, the low recovery values and the high salinity of water produced at the surface (Fu & Dehghanpour 2020; Jia et al., 2013; Zhou et al., 2016) prove that a considerable amount of the fracturing fluid remains in the subsurface and is likely to infiltrate aquifers.

The time needed for the fluid migration to occur depends on the average permeability between the formation pathway linking the HF source and the aquifer, hence, the HF fluid might only be detected in drinking water after decades of HF operations. This makes the environmental concern of the fate of fracking fluids a long-term issue. To further validate such environmental concerns, studies have shown that the hydraulic fractures may intersect pre-existing ones which creates a complex network of hydraulic conduits that promote contaminant transport to aquifers and groundwater wells (Llewellyn et al., 2015; McClure, 2014; Osborn et al., 2011; Vidic et al., 2013). From here, the mechanisms of fracking fluid migration should be understood, and the timescales associated with their infiltration to aquifers should be quantified based on the hydro-geologic conditions to propose and implement risk mitigation plans. For example, Birdsell et al. (2015) simulated the migration of hydraulic fracturing fluid injected through a horizontal well into the Marcellus shale reservoir and showed that, after 20 years, 68% of the injected fluid was produced by the well, only 0.1% reached an overlying aquifer, and the remaining fraction was distributed in the subsurface. Taherdangkoo et al. (2019) modeled fracturing fluid transport from a low permeability shale reservoir to an overlying shallow aquifer via a leaky abandoned well. They showed that 67% of the injected fracturing fluid was recovered and 0.02% reached the aquifer after 30 years.

Extensive simulations have been proposed to model hydraulic fracturing operations (Khadijeh et al., 2022), fracturing fluid migration in the subsurface, and to investigate how different formation parameters affect fluid flow in the subsurface (Almulhim, 2014; Aseeperi, 2015; Birdsell et al., 2015; Fakcharoenphol et al., 2013; Figueiredo et al., 2017; Ghanbari & Deghanpour, 2016; Li et al., 2012; Liu et al., 2019;

Pfunt et al., 2016; Sarkar et al., 2016; Seales et al., 2017; Wang et al., 2017; Yarushina et al., 2013; Yu et al., 2016; Zanganeh et al., 2015). These studies provide a good understanding of fracturing fluid distribution post-fracking and of the several phenomena behind the low fracking fluid recovery. According to Birdsell et al. (2015), the different factors affecting the flow of fracturing fluid after injection are the overpressure of the reservoir, increased pressure in the shale due to the injection of the fluid, presence of permeable pathways and their characteristics, buoyancy of the hydraulic fracturing fluid, topographically driven flow, and imbibition. Furthermore, Liu et al. (2019) showed that the properties of the induced fractures influence the recovery rates, whereby the higher the density of fractures, the lower the fracking fluid flow-back rate and hence the lower the recovery.

The presence of fluid flow pathways in the subsurface is illustrated by two proven phenomena; fracturing fluid leakage through complex fracture systems (Li et al., 2007; McClure, 2014), and contaminant migration into aquifers (Myers, 2012; Gassiat et al., 2013; Birdsell et al., 2015; Llewellyn et al., 2015). So, from a geological point of view it's essential to study the geological features of targeted formations in search of potential hydraulic conduits that can serve as pathways for fracturing fluid migration to aquifers and fracture network complexities dominating fluid flow in fractures. The term "fracture" is often used in the literature to describe all discontinuities in the rock (e.g. fault, fissures, joints, and cracks) (Ren et al., 2017).

Shales are sedimentary rocks of low permeability composed mainly of clay (Li et al., 2020; Myers, 2012). In unfractured shales, porous flow is almost negligible because of the low matrix permeability. However, due to their considerably higher permeability in comparison to matrix permeability, fractures are mainly the preferential

pathways for fluids making fracture flow the prevailing flow in fractured rocks (Khang et al., 2004; Myers, 2012; Ren et al., 2017). Particularly, fluid flow mainly takes place via faults (Ishii, 2017) and the majority of fracturing fluid leakage (about 90%) takes place through natural fractures (Li et al., 2007). Deriving which fluid pathways in the fractured rock are the preferential ones depends on the permeability, which is influenced by the mechanism of deformation. Faults are proven to have the most impact on fluid flow and contaminant transport (Hirono et al., 2003).

When compared to porous flow, fracture flow exhibits more heterogeneity, anisotropy, and irregularity due to the added complexity of its fracture systems. This complexity is reflected by the various distributions, scales, and densities of discontinuities in the rock mass. Moreover, fractures exhibit heterogeneity in shape, size, aperture, and spacing (Ren et al., 2017). Furthermore, heterogeneity of the hydraulic properties (e.g. permeability) of fault zones and their structural complexity give them the ability to serve as conduits allowing fluid flow in cases of high permeability (Hsu et al., 2022).

Several studies have also discussed the relation between shale properties and fracturing fluid retention mechanisms. In their review of the impact of water chemistry on shale properties, Khan et al. (2021) revisited five main mechanisms that affect the shale's flow potential. These mechanisms, resulting from the fluid-solid interaction at the shale surface, are shale softening, mineral precipitation, mineral dissolution, wettability alteration, and fines migration. The experiment of Abdulelah et al. (2018) on shales from the Batu Gajah and Kroh formations in Malaysia, showed that higher fluid retention is observed in the shale that has a higher clay content and lower total organic content (TOC). This behavior is expected due to the hydrophobic nature of the organic

matter and the hydrophilic nature of the clay. In contrast, when Yongjun et al. (2018) performed experimental studies on the phenomena leading to the low flow-back recovery in marine shales, they concluded that the fluid retention is primarily caused by adsorption and not by swelling of the shale. This is due to the fact that the fluid does not reside between the clay mineral layers, but it gets adsorbed at the surface of micro-fractures induced, where an 80% decrease in fracture width lead to a 35% increase in the water adsorption rate yielding a higher fluid retention and lower flowback.

Available literature concerning fracturing fluid flow-back provides a general understanding of the possible reasons behind the low recovery. It states that these reasons include, but are not limited to, water imbibition by spontaneous capillary forces into the shale matrix, fluid leakage into the formations surrounding the shale, and its entrapment in the complex fracture networks resulting from the fracturing operations (Fakcharoenphol et al., 2013; King, 2012; Li et al., 2007; Liao et al., 2019; Wang et al., 2017; Yang et al., 2015; Yarushina et al., 2013). The studies on fluid migration focus mainly on its possible upward migration through simple networks where only one fault or abandoned well is considered (Birdsell et al., 2015; Gassiat et al., 2013; Kissinger et al., 2013; Lange et al., 2013; Llewellyn et al., 2015; Myers, 2012; Pfunf et al., 2016; Taherdangkoo et al., 2019). Moreover, issues like well interference in multi-lateral horizontal well fracturing operations (He et al., 2020; Yu et al., 2016), pressure-dependent permeability (Figueiredo et al., 2017; Liao et al., 2019), and complex networks of hydraulic conduits have been left out from the analysis although they are of significant influence on the fracturing fluid flow-back. Also, extending the simulation time (beyond 20 years) can reveal different conclusions from a sustainability perspective, especially that fluid seepage and migration is a relatively slow process.

In this study, the hydraulic fracturing fluid transport is numerically modeled, and a thorough parametric study is performed to assess the effect of chosen parameters on the fluid flow.

We address unanswered questions related to the effect of the complexity of the subsurface fracture network and its evolution on the flow back rates. We model the fracture networks resulting from the intersection of the hydraulic fractures and one permeable conduit in the overlying layers, and then extend it to model an intersecting network of several hydraulic pathways in the underlying formations. The hydraulic fracturing fluid flow-back is estimated in a case of multi-well pad hydraulic fracturing operation while taking into consideration the different degrees of fracture network complexity and the permeability changes caused by pressure variations.

# CHAPTER 2

## LITERATURE REVIEW

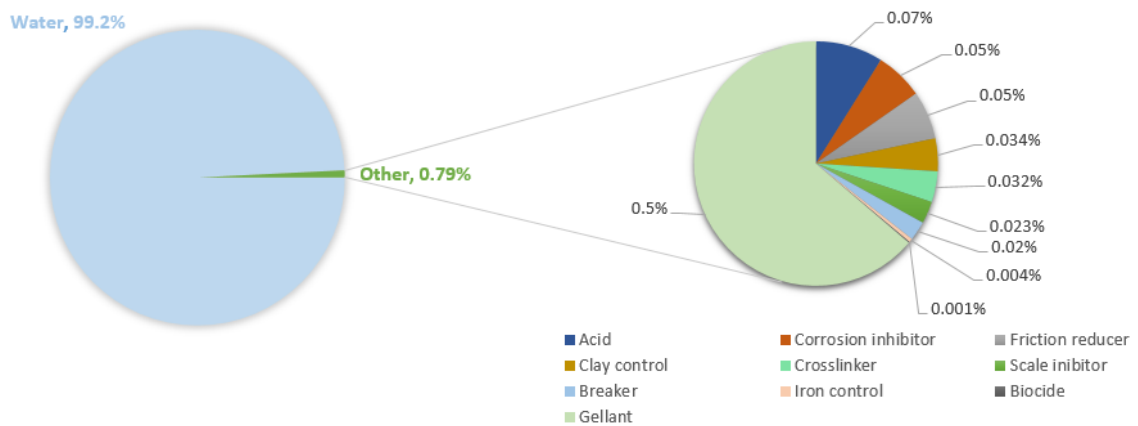
### 2.1 Environmental Impact of Fracturing Fluids

#### 2.1.1 Fracturing Fluid Composition

Fracturing fluid is the fluid used in hydraulic fracturing operations to create hydraulic fractures in targeted tight formations to develop pathways for the trapped hydrocarbons. The fracturing fluid is a mixture of the base-fluid (i.e. water, oil, foam, or acid) and other chemicals required to enable the success of the fracturing process. As illustrated in Figure 1, some additives constituting the fracturing fluid are clay stabilizers, friction reducers, corrosion inhibitors, and many more. The selection of the suitable fluid composition depends on the results anticipated from the fracturing job and the formation in question (Shah et al., 2015).

**Figure 1**

*Water Based Fracturing Fluid Composition (reproduced from Shah et al., 2015)*



### **2.1.2 Associated Risks**

Environmental risks linked to fracturing fluid usage are on the top of the environmentalists' list of concerns when it comes to warning about the drawbacks of hydraulic fracturing. Specifically, environmental hazards related to groundwater contamination by additives in the fracturing fluid. Contamination might be the result of aboveground incidents (e.g. spillage during transport) or fluid's infiltration into aquifers through the subsurface layers (Kreipl & Kreipl, 2017).

Shah et al. (2015) considered the tracking of the motion of the fracturing fluid as a pre-requisite to assessing the environmental hazards associated with it. Similar to Kreipl's classification, they were able to categorize the potential risks into two main categories: (i) Surface risks, and (ii) downhole risks.

The category of surface risks includes, but is not limited to, fracturing fluid spill during its transport, and fluid leakage from storage pits. One of the most alarming impacts of these events is the possible contamination of subsurface aquifers.

As for the downhole risks, they are summarized by the possible scenarios of upward fracturing fluid migration towards drinking water aquifers. Although such scenarios are of low probability, cases of drinking water contamination by fracturing fluid have been reported (see Table 1). This migration can take place through shallow leaky casings near the aquifers, due to poor cementing jobs that lead to generation of channels thus creating a flow path for the fracturing fluid to infiltrate into unfavorable zones, or as a result of the intersection between the initiated fractures and pre-existing faults (Shah et al., 2015). In addition, Ingraffea et al. (2014) discussed well's integrity and its association with leakage of liquids and/or gases towards groundwater aquifers in case of faulty casings installment.

**Table 1**

*Drinking Water Contamination Incidents Linked to Hydraulic Fracturing Operations in the United States (Birdsell et al., 2015)*

Location	Date	Chemicals Detected	Possible Reason
Jackson County, West Virginia	1982	Fracturing fluid gel	Migration through nearby gas wells
Garfield County, Colorado	2004	BTEX	Poor wellbore integrity (i.e. improper cementing job)
Pavillion, Wyoming	2008	Fracturing fluid components	Short distance between aquifer and well.

On the other hand, Mrdjen and Lee (2015) focused in their study on one of the issues that has been addressed in a lesser degree in the literature when compared to other concerns related to hydraulic fracturing operations, which is the threat the hydraulic fracturing-related chemicals pose to human health when they contaminate surface water bodies considered as drinking water sources. Surface water bodies in question include rivers and streams, which are exposed to serious hazards during the transport of stimulation fluids due to the considerable chance of undesirable incidents and spills (Mrdjen & Lee, 2015).

To enrich the literature, DiGiulio and Jackson (2016) evaluated the impact of well stimulation on underground drinking water sources based on the investigation initiated by the Environmental Protection Agency (EPA) in 2008 of the reason behind the reported changes noticed in odor and taste of drinking water produced from

domestic wells located in the Pavillion Field, Wyoming. To be able to examine possible upward migration of chemicals linked to hydraulic fracturing, EPA resorted to installing two monitoring wells and sampling them. Sampling results revealed considerable concentrations of some fracturing fluid constituents and/or corresponding degradation products in one or both of the monitoring wells. Some of the organic compounds detected were trimethylbenzene, naphthalene, methylnaphthalenes, alkylbenzenes, tert-butyl alcohol, diethylene glycol, nonylphenol, and octylphenol. The detection of these compounds gives extra credibility to the proposed scenario of the upward migration of fracturing fluid constituents to drinking water sources via pathways in the subsurface. Before getting into the details of the case investigated by EPA, DiGiulio and Jackson (2016) were able, through examination of other incidents that have occurred throughout the previous decades in the Pavillion field, to deduce that the solute transport of fracturing chemicals to underground drinking water sources in this field might have occurred in response to several phenomena including: (i) leak-off through the fractures, (ii) lithologic heterogeneity and the presence of permeable layers that allow fracturing fluid's migration, (iii) casing failure that facilitates fluid seepage, and (iv) injection of fracturing fluid near or directly into the drinking water sources.

The main reason behind the relentless cautioning by environmentalists regarding the threat of fracturing fluid on groundwater's integrity is the serious hazards the chemical additives pose on human health and wellbeing. Fracturing fluid chemicals might have implications on the sensory organs, brain and nervous system, respiratory system, and immune system. However, the acuteness of these effects of course depends on the degree and way of exposure to the chemicals.

In their attempt to evaluate potential health risks caused by the chemicals present in hydraulic fracturing fluids, Elliot et al. (2016) collected data from different databases for 925 of disclosed chemicals usually added to the fracturing fluids. Specifically, the databases were scanned for information regarding reproductive and developmental toxicity. Out of the 925 constituents, toxicity-related information was accessible for only 194 constituents (21%) with 61 chemicals having both reproductive and developmental toxicity data available (Figure 2). As for the degree of association with harmful effects, Figure 3 shows that 80% of the chemicals with available reproductive toxicity data were probably linked to reproductive toxicity and 46% of the chemicals with available developmental toxicity data were probably linked to developmental effects.

**Figure 2**

*Toxicity Information for the 194 Fracturing Fluid Constituents with Accessible Data Out of the 925 Constituents Studied (Elliot et al., 2016)*

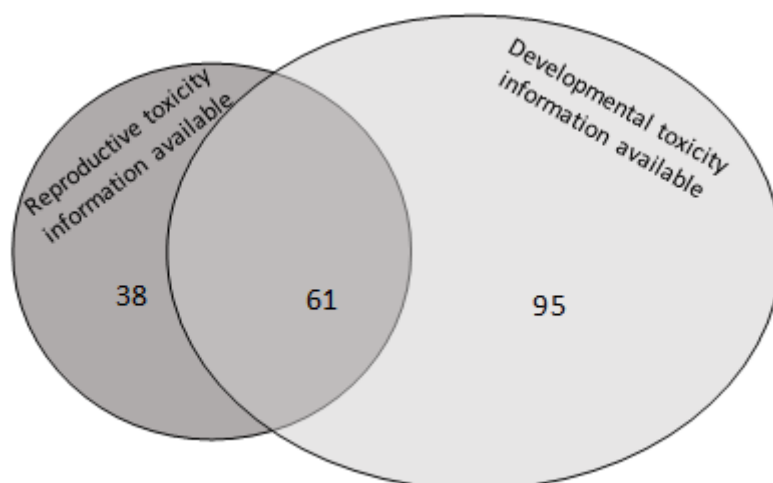
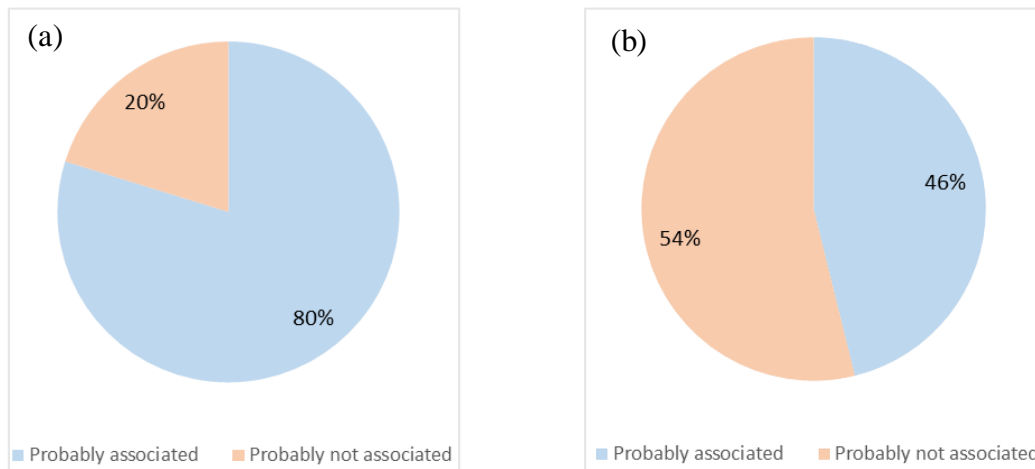


### Figure 3

*Percentage of Chemicals Associated with (a) Reproductive Toxicity, and (b) Developmental Toxicity, Based on the Number of Chemicals with Available Toxicity Data (Elliot et al., 2016)*



In light of the facts and analyses presented in this section, it's inevitable to point out that even in the case of not reaching the underground drinking water sources as a result of migrating through permeable layers, the hydraulic fracturing fluid remains toxic posing a risk to human health in cases of accidents or usage of fluid with additives' concentrations higher than the limits set by acts concerned in monitoring drinking water quality (Kreipl & Kreipl, 2017). Adding to that, the fact that not all operators disclose the compounds of the fracturing fluids used and the ambiguity and limited availability of toxicity-related information make the process of investigating the environmental impacts of fracturing fluid a more critical one. Also, the outcome of such studies must provide insights about possible threats posed by the fluid during and after fracking operations, because the recognition and examination of the resulting hazards usually requires several years (Murphy, 2020).

Consequently, monitoring and simulating the transport of the fracturing fluid in the subsurface and studying its fate –for long periods of time- becomes a must (Elliot et al., 2016). The necessity of this requirement is validated by the incomplete return of the fluid to the surface where low fracturing fluid recovery values are reported (Birkle 2016; Zhou et al., 2016; Osselin et al., 2018), proving that a considerable portion of the fluid actually remains in the subsurface with a potential of infiltrating into drinking water sources like the case in the Pavillion field, for example. Therefore, the next section of this chapter is dedicated to discussing the fate of the fracturing fluid and the parameters/phenomena affecting its flowback.

## **2.2 The Fate of the Fracturing Fluid**

### ***2.2.1 Parameters Affecting Flowback***

Load recovery is the term used to describe the percentage of injected fracturing fluid that is produced back post hydraulic fracturing treatment where the wells produce considerable volumes of the fracturing fluid (mainly water) for several days before oil/gas breakthrough takes place and major fraction of this recovery usually occurs during the first three months of production (Zanganeh et al., 2015). Fracturing fluid flow-back is usually low and the expected recovery is about 25% in Marcellus shales during the first month of flow-back (Henderson et al., 2011). The fracturing fluid (slick-water) flow-back prior to hydrocarbon production is essential for the success of hydraulic fracturing, and the low recoveries recorded are considered as an alert for the environmentalists interested in tracking the migration of the contaminants that remain in the subsurface post-production. Thus, the correlation between the load recovery and different parameters, like the shut-in period, and fracture network complexity, is of

great interest and occupies a considerable portion of the studies investigating fluid flow-back recovery, as demonstrated in Table 2.

**Table 2**

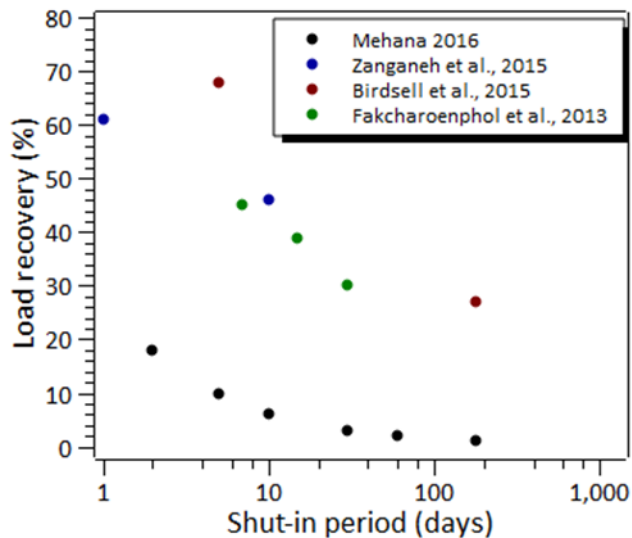
*The Correlation Between Different Parameters Studied in the Literature and the Load Recovery*

Parameter studied	Relation with load recovery	References
Shut-in period	Negatively correlated	Fakcharoenphol et al.(2013) Zanganeh et al. (2015) Birdsell et al. (2015) Ghanbari and Dehghanpour (2016) Mehana (2016) Seales et al. (2017)
Natural fracture density	Negatively correlated	Mehana (2016) Wang et al. (2017) Liao et al. (2019)
Fracture closure	Negatively correlated	Liao et al. (2019) Liu et al. (2019)
Rock wettability	Hydrophobicity: positively correlated	Jia et al. (2013) Sarkar et al. (2016)
Hydraulic fracture permeability	Positively correlated	Birdsell et al. (2015) Zanganeh et al. (2015)
Salinity of brine	Negatively correlated	Mehana (2016) Wang et al. (2017)
Reservoir pressure	Positively correlated	Jia et al. (2013) Wang et al. (2017)
Fracture network complexity	Negatively correlated	McClure (2014) Ghanbari and Dehghanpour (2016) Liao et al. (2019)

Figure 4 presents the correlation between the load recovery and the shut-in period. Data points are derived from numerical simulations presented in the literature. It's clear that extending this period leads to a reduction in the load recovery, as deduced in the different studies referred to in Figure 4. It should be noted that although in each simulation different formations were studied and different modeling parameters were used, the trend of data points corresponding to the same study (i.e. same models and same modeling conditions) prove the mentioned correlation between shut-in period and load recovery.

**Figure 4**

*Load Recovery vs Shut-in Periods in Several Studies*

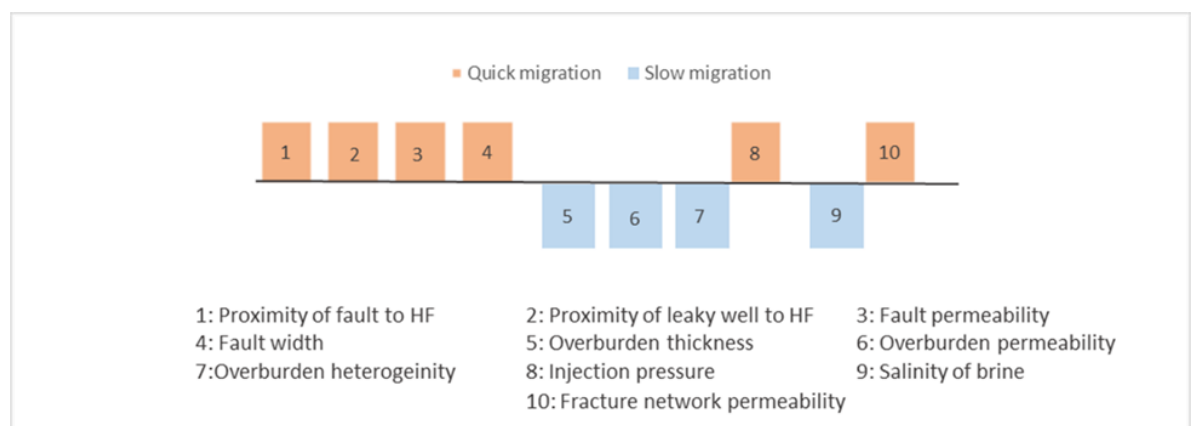


The issue of possible aquifer contamination is directly related to low fracturing fluid flow-back rates, because a hydraulic communication, which is made possible in the subsurface due to hydraulic fractures intersection with the previously existing permeable pathways (e.g. faults, abandoned wells), distinctly contributes to the low

recovery values. So, several studies investigating this upward flow indirectly gave insights about the fate of the un-produced fluid (Arthur et al., 2008; Birdsell et al., 2015; Gassiat et al., 2013; Kissinger et al., 2013; Myers, 2012; Osborn et al., 2011; Pfunf et al., 2016; Taherdangkoo et al., 2019; Taherdangkoo et al., 2017). For example, Birdsell et al. (2015) and Taherdangkoo et al. (2017) focused on the need to understand the transport of the injected fracturing fluid to make sure that shallow drinking water aquifers are not contaminated since the intersection between created fracture network and preferential pathways might act as flow pathways. Moreover, we can see in Figure 5 how some conditions control the speed of this migration as per the literature, we can notice that the shorter the distance is between the fault and the hydraulically fractured region, for instance, the quicker the migration occurs.

**Figure 5**

*The Speed of Fluid's Upward Migration as a Function of Increase in Different Parameters Studied in the Literature ( Gassiat et al., 2013; Pfunf et al., 2016; Taherdangkoo et al., 2017; Taherdangkoo et al., 2019)*

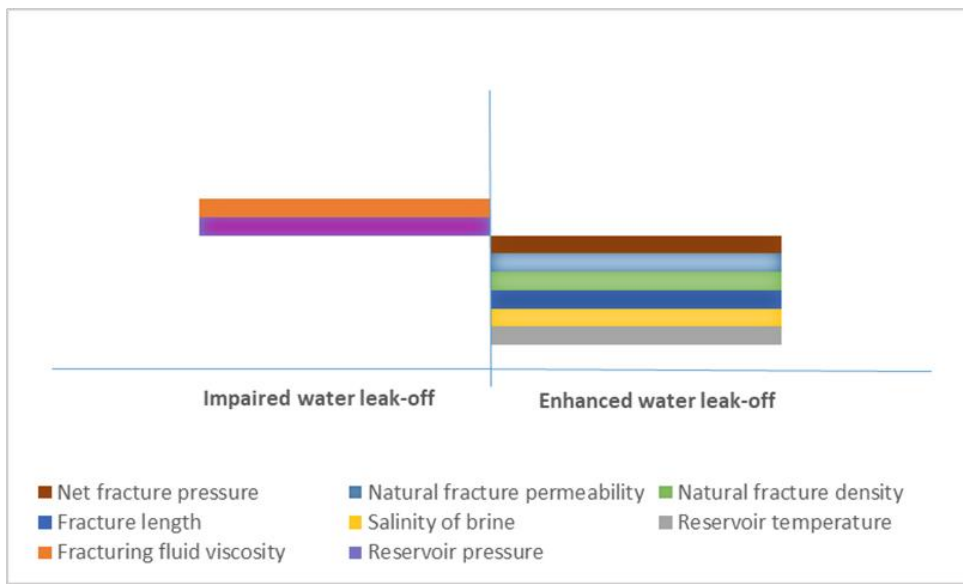


In tight reservoirs, complex fracture networks are created by utilizing multi-stage hydraulic fracturing and horizontal wells, where other reasons for such low flow-back percentages are believed to be the retention of the fluid in these fractures and its leak-off through them into the matrix (Li et al., 2007; McClure, 2014; Wang et al., 2017; Yarushina et al., 2013) and flow-back data analysis strongly supports this belief (Liao et al., 2019). The evaluation of fracturing operations and forecasting of the well productivity require fracture characterization. However, due to the unknown density and reactivation of the natural fractures in shales, it is hard to quantitatively characterize the complex fracture networks (Liu et al., 2019).

Fracturing fluid leakage into the formation through the main fracture is known as the fluid loss. Several models have been dedicated to simulating fluid loss (Li et al., 2007; Wang et al., 2017; Yarushina et al., 2013; Yang et al., 2015) and this stems from the importance of fluid loss rate in both the treatment design, and the fracture geometry determination in naturally fractured reservoirs (Li et al., 2007). The mechanism of water leak-off is influenced by several properties, as shown in Figure 6, where an increase in natural fracture density for example induces an enhancement in the water leak-off. The relation between pressure and fluid leak-off into the formation is best represented in the model when pore compressibility and porosity-dependent permeability are taken into consideration. In real applications, the fracturing fluid leak-off is likely to take place, which negatively impacts the efficiency of the fracturing job (Yarushina et al., 2013).

**Figure 6**

*The Effect of Increase in Different Parameters Studied in the Literature on Water Leak-off ( Ghaderi et al., 2018; Li et al., 2007; McClure, 2014; Wang et al., 2017; Yang et al., 2015)*



Due to the heterogeneities that might be encountered in the subsurface, it is essential to study how hydraulic fracturing is performed in complicated geological settings to optimize hydrocarbon recovery from shale reservoirs. Complex geological settings might include complex in situ stress field, pre-existing faults and bedding planes, spatial variability of rock mass properties, local heterogeneities (Figueiredo et al., 2017).

### **2.2.2 Effect of Fracture Network Complexity on Load Recovery and Oil/Gas Production**

It has been proven in the literature and through microseismic monitoring that hydraulic fracturing creates a fracture system with a considerable degree of complexity

due to the presence of generated hydraulic fractures, reactivated and preexisting natural fractures, yielding a large spectrum of fractures' dimensions. Fracture network complexity affects both the load recovery and hydrocarbon fluid production rates (Ghanbari & Dehghanpour, 2016; Liao et al., 2019; Liu et al., 2019).

Ghanbari and Dehghanpour (2016) utilized flowback data of 18 hydraulically fractured wells in the Muskwa, Evie, and Otter Park formations in the Horn River Basin, Canada, to be able to assess the effect of several parameters, including but not limited to fracture network complexity, on production of water and gas. They were able to classify the wells based on their flowback efficiency and produced gas volumes during the first 72 hours of production into two categories: High gas and low water production, and Low gas and high water production.

The degree of complexity has a direct effect on flow of fluids and hence on the recovery of these fluids (i.e. both fracturing fluid and hydrocarbon fluid). So, a different fracture system is proposed for each category to clarify the reason behind the production trends observed.

- High gas and low water production category:

During the injection phase, fracturing fluid and proppants fill the hydraulic fractures while the natural fractures are usually mostly filled with the fluid only, thus the hydraulic fracture's aperture becomes larger than that of the natural fractures. So, when production takes place after the shut-in phase most of the water in the hydraulic fractures gets produced back to the surface while a great fraction of the water in the natural fractures gets trapped in them. This is attributed to the higher conductivity of the hydraulic fracture and the tortuosity of the natural fractures. During shut-in, the trapped water imbibes into the formation and displaces the gas in the matrix so this gas

flows into the fractures (hydraulic and natural) and gets produced during the first period of flowback. There might be gas that has been trapped in the natural fractures before the initiation of fracturing job, but during the shut-in period it gets liberated and flows to the hydraulic fractures due to gravity segregation and pressure drawdown. So, it can be deduced that the more complex the fracture network generated is, the larger the contact surface is between the shale matrix and the fractures and hence the stronger the imbibition is. This leads to lower load recovery and higher gas production rates during the early times of production.

- High water and low gas production:

The production trend in this case can be linked to a fracture system that is less complex than the system proposed earlier, where less natural fractures are assumed to exist. Such fracture systems yield smaller contact surface which in turn hinders water imbibition into the matrix and facilitates the accumulation of the fracturing fluid in the hydraulic fractures. Hence, during the shut-in period less gas builds up in the fracture system leading to higher load recovery and lower gas production rates during the early time of production.

To validate the reasoning behind the proposed fracture systems corresponding to the field flowback data available, Ghanbari and Dehghanpour (2016) numerically modelled a flowback process to evaluate the impact of fracture network complexity and other parameters on fluid production rates. In their model, they included natural fractures and to account for complexity they introduced a complexity index that is dependent on the volume of both the hydraulic and natural fractures. They varied the index by varying the number of natural fractures in the model while keeping the volume of hydraulic fractures constant. Simulation outcomes indicate that a higher index, representing a

more complex fracture network, curbs the load recovery and boosts gas production. This can be attributed to the fact that increasing the density of natural fractures generates a larger contact surface area between the shale matrix and fractures. The larger the surface area, the greater the fraction of water that imbibes into the shale matrix displacing the gas that gets accumulated in the fractures and gets easily produced by the well.

Due to the uncertainty of the characteristics of the complex fracture systems created during hydraulic fracturing operations and the great effect they have on water entrapment and thus on production from the well, Liao et al. (2019) developed a series of numerical models to assess the influence of parameters including fracture density, heterogeneity, and compressibility. When accounting for the compressibility of the fractures during shut-in and production, water load recovery decreases and breakthrough time of the oil is delayed in comparison to cases of ignoring the stress dependence of fractures. During shut-in and flowback, if fracture compressibility (i.e. closure) is ignored then while the water that accumulated in the hydraulic fracture gets produced, the fraction of water that's near the hydraulic fracture will be able to flow into the fracture and be produced by the well yielding an improved load recovery. On the other hand, if compressibility is taken into account then the fractures are expected to re-close due to pressure changes, thus after the depletion at the level of the fractures, the fraction of water that's near the fracture will imbibe into the surrounding matrix. As for the oil production, accounting for fracture compressibility also curbs it. This can be explained by tracking the water saturation vs time near the natural fractures. As stated earlier, the closure effect of the fracture results in stronger imbibition into the matrix and hence higher water saturation which leads to lower relative permeability to

oil hindering its mobility and hence we observe the delayed breakthrough time and lower oil production volumes.

Similar to the approach followed by Ghanbari and Dehghanpour (2016), Liao et al. (2019) accounted for complexity in their models by introducing the same complexity index used by Ghanbari and Dehghanpour (2016). As expected, their results showed that as natural fracture density increases, fracturing fluid recovery decreases and oil production increases. This is a consequence of the enhanced contact surface area between the matrix and the fractures which promotes/boosts fracturing fluid leak-off. Water retention might be highly controlled by the natural fracture heterogeneity because the opening of fractures during injection and their closure during shut-in and production is not uniform. Different degrees of heterogeneity (i.e. weak, medium, and strong) are implemented in the model through the variation of permeability coefficients. Strong heterogeneity of natural fractures promotes fracturing fluid loss into the reservoir, and leads to high saturation of water in the closed areas of the natural fracture. This leads to lower fracturing fluid recovery when compared to the case of homogeneity. Although heterogeneity also reduces oil production, the effect it has on hydrocarbon fluid production is minimal when compared to other properties.

Matching field data with simulation results gives information about fracture characteristics like conductivity, half-length, and density (Liu et al., 2019). So, for the purpose of fracture characterization and to generate correlations between fracture characteristics and production rates yielded post hydraulic fracturing, Liu et al. (2019) first ran a numerical simulation and then did a history matching based on production data reported for two shale gas wells (WY and YY) fractured in the Longmaxi formation, China. Firstly, simulation results showed that a higher conductivity of the

hydraulic fractures leads to a higher water recovery. However, it results in a lower gas recovery. Similar effect is created by the increase in the length of the hydraulic fracture, but in a lesser degree. Contrarily, both water and gas accumulated volumes decrease when the closure coefficient of the natural fracture is amplified. Secondly, the fact that simulated production rates of water and gas matched with the rates provided from field data serves as added support to the correlations proposed by their simulation outcomes concerning fracture network properties and fluids recovery (i.e. water and gas).

Similar to studies discussed earlier, Yongjun et al. (2018) also derived a negative correlation between fracture network complexity and flowback recovery and a positive one between complexity and gas rates. Their conclusions were based on flowback data, including water and gas rates, taken from 9 wells from the Zhaotong, Weiyuan, and Changning blocks in China.

To sum up, phenomena explained in this section thoroughly describe fluid flow in complex fracture networks and the probable correlations existing between different fracture properties (e.g. fracture compressibility, hydraulic fracture conductivity, and natural fracture density) and production rates.

### ***2.2.3 Seismicity Induced by Fluid Diffusion***

#### **2.2.3.1 Induced Seismicity in the Western Canada Sedimentary Basin**

The surge in the number of earthquakes recorded in the Western Canada Sedimentary Basin (WCSB) and in their magnitudes is strongly attributed to hydraulic fracturing processes (Schultz et al., 2018). A spatial and temporal link has been developed between the rise in seismic activity during the last decade in western Canada and the hydraulic fracturing operations in that region (Hui et al., 2021). Especially in

the Fox Creek area, Alberta, where induced seismicity yielded earthquakes with magnitudes that are considered among the highest globally among earthquakes related to hydraulic fracturing (Hui et al., 2021; Schultz et al., 2018). Moreover, the proposed correlation between induced seismicity in the upper Devonian Duvernay formation and hydraulic fracturing is supported by the provided sequences of earthquakes in the region (Bao & Eaton 2016).

With the increase in the magnitudes of earthquakes linked to hydraulic fracturing operations, regulators emphasize the importance of monitoring induced seismic activity near fracking sites in western Canada and the United States (Karimi et al., 2018). By screening available data sets from western Canada, Karimi et al. (2018) concluded that this seismicity is usually a result of alterations in the loading conditions that are caused by the injection of highly pressurized fracturing fluid in the subsurface near existing faults that are unmapped.

For instance, Bao and Eaton (2016) combined available injection data with recorded timing and allocation of earthquakes in a shale play in Canada that is known to be seismically active, and generated an earthquakes distribution that is concentrated both spatially and temporally near well pads where hydraulic fracturing is taking place. Where the largest earthquake recorded in this region followed the injection along the fault connecting the injection zone and the basement by a few weeks.

In response to the rise in seismic activity in Fox Creek, Alberta, since 2013, Schultz et al. (2018) used data from a hydraulic fracturing database to study the correlation between the occurrence of earthquakes and operational parameters (e.g. injected fracturing fluid volume). Accordingly, they deduced that, in the Duvernay formation in specific, the dominating factor that has a direct positive correlation with

the number of recorded seismic events is the injected fluid volume. Reliable data about the injected fluid volume serves as valuable input for models aiming to predict earthquakes rates and corresponding magnitudes in this region since this piece of data provides insights about the expected fluid volume that might diffuse and cause fault activation.

Furthermore, based on a case study in Fox Creek, Alberta, Hui et al., 2021 were able to quantify pore pressure diffusion by conducting a coupled fluid flow-geomechanics simulation. Established on the basis of the 3D seismic data of the studied region, three identified faults were included in the simulation. Modeling hydraulic fracture propagation yielded a relation between the injected fluid volume, hydraulic fracture half-length and induced events. It was noted that the half-length and injected volume are positively correlated to each other and to induced seismicity, and the increase in one of them leads to the increase in the other, hence enlarging both the number and magnitudes of the induced earthquakes. Accordingly, the hydraulic communication between the faults and the fractured region is affected by the operational parameters which in turn affects the pore pressure diffusion that causes the activation of the faults. Moreover, it's worth noting that the hydraulic fracture permeability is considerably higher than the formation permeability, implying that this difference in permeability promotes the seepage of fracturing fluid from the fractures into the surrounding strata.

The reason behind the triggering of the earthquakes in this case study can be summarized as follows, the injected fracturing fluid provoked the fault seismic slip by its diffusion through the induced fractures towards the faults (Hui et al., 2021).

Moreover, the damage zones of the existing faults, which are of high permeability,

enhanced the hydraulic connectivity among these faults and the fluid diffusivity, intensifying pore-pressure variations that lead to fault re-activation.

Similarly, Shapiro and Dinske (2009) noted that spatially, the microseismicity is usually clustered near the hydraulic fractures. Also, that tracking the fracture growth shows that when the injection pressure is increasing the fractures open and when it's dropping the fractures close. Although this behavior is expected, a fluid injection over a long period of time promotes the process of fluid loss into the surrounding formation. When fluid injection stops, the main trigger of induced seismicity becomes the pressure release in the fractured region.

In their attempt to generate an association between operational parameters and induced seismicity in the Duvernay formation, Bao and Eaton (2016) gathered data of a period of four months for six well pads where hydraulic fracturing operations were carried out in this area and through this data they were able to cover all the fracturing activities taking place in this region during this time period. The clusters of recorded seismic events were only about 2 km laterally away from the fractured wells with few events being detected between these clusters.

They plotted the available data of both the average daily injection pressure and the cumulative injected fluid volume and compared it with recorded seismicity and corresponding magnitudes of certain clusters. This comparison showed that the event with the highest magnitude among the recorded ones took place during the flowback period, two weeks after fracturing commenced at one of the studied well pads.

Flowback recovery reported at this well pad was as low as 7% indicating that a large fraction of the fluid (~ 93%) remains in the subsurface with the potential of hydrologically communicating with the fracture network and pressurizing the existing

fault. Activation of the fault zone occurred repeatedly for few months following the hydraulic fracturing completion. This activation was in unison with the pore pressure diffusion into the fault zone.

Consequently, they deduced that the two main phenomena that can be considered as triggers for the induced seismicity felt in this region are the stress changes as a result of fracturing the tight formation and the fluid diffusion along faults. However, the effects of pore pressure changes are more persistent than those of stress changes leading to the pressurization of the fault which in turn generates seismicity.

#### 2.2.3.2 Induced Seismicity in the Sichuan Basin, China

Due to the importance of performing a spatial and temporal study of seismicity in the Sichuan Basin in China, Sheng et al., 2022 compiled seismic data recorded over a period of 1 year in the Weiyuan shale gas block into a catalog. They worked on detecting and relocating 18,663 recorded earthquakes in the Weiyuan region. Monitoring the spatial and temporal evolution of the earthquakes showed that the majority of the events were clustered at locations relatively near the injection well pads (within 5 km from the platforms) and that the faults serve as permeable pathways that allow fluid flow. The fact that the faults that are reactivated promote fluid flow through them facilitates the triggering of earthquakes away from fracturing sites/fractured wells.

While waste-water is usually injected into deep formations in the United States, a different approach is taken in the Weiyuan region where wastewater is accumulated at the surface and purified for the purpose of recycling (Liu et al., 2020). Thus, the scenario of seismic activity being triggered due to injection of wastewater is of low

probability in the Weiyuan region. This fact serves as additional confirmation for the link between hydraulic fracturing operations and induced in the examined region. Furthermore, to study the triggering mechanisms, Sheng et al. (2022) modelled earthquakes migration as processes of fluid diffusion. Hydraulic diffusivity values used in the simulation correspond to low permeability values of the shale. Low permeability values of the tight shale formations and the fact that hydraulic fractures only extend for a couple hundred meters from the fractured well don't promote pore pressure diffusion to long distances. However, in this case study most events were clustered within 5 km from the fracturing sites and many of the events that are near the well pad were at a distance larger than 1 km from it. So, a reasonable conclusion is that the faults that are connected with the fractured wells via the induced hydraulic fractures serve as permeable pathways for fluid flow allowing for triggering of events at distances far away from the injection wells.

In addition to the reasoning provided above, Sheng et al. (2022) noted that fault-valve behavior might be one of the reasons behind the induced seismicity. During injection, the fluid might have been accumulated in the fault-valve leading to a considerable pressure difference, then when rupture occurred (i.e. post-failure) a rapid fluid discharge took place triggering seismicity. This behavior leads to enhancement in the permeability of the fault zone allowing the initiation of events at long distances from injection wells.

A similar approach was taken by Tan et al. (2020) to investigate the proposed correlation between the growing induced seismicity recorded in the southern Sichuan Basin in China and the shale exploitation activities in the region. The monitoring data retrieved from a local seismic network near targeted formations helped them prove this

close correlation by comparing the time when the earthquakes occurred with the stimulation schedules of the well pads studied.

They based their study on the injection data available for two well pads (N5 & N7) in the Sichuan Basin. The chronological distribution of seismic activity surrounding N5 demonstrated a clear correlation between hydraulic fracturing and earthquakes initiation, where only few days separate the start of fracturing operations and the recording of the first earthquake and there's also a synchronization between the timing of recorded earthquakes and stimulation activities. On the other hand, fewer earthquakes were recorded around N7 and this is attributed to the fact that no blind faults exist beneath this pad. The different deductions agree with the flowback rates associated with each well pad, where 45% and 40% rates are achieved for pads N7 and N5, respectively, hinting to the higher potential of fluid storage beneath N5 when compared to the space beneath N7.

Hence, one of the main phenomena causing fluid induced seismicity is concluded to be the fluid diffusion- following fluid injection- where the fracturing fluid reaches the faults through hydraulic communication between faults and hydraulic fractures. This leads to the reactivation of pre-existing faults where pore pressure increase that takes place during hydraulic fracturing is enough to initiate a slip on faults triggering earthquakes. (e.g., Bao & Eaton 2016; Tan et al., 2020)

Conclusions derived from the case studies and simulations presented in this subsection might seem redundant but the fact that several authors report that fluid diffusion is one of the main phenomena behind induced seismicity near fracturing sites adds credibility to the hypothesis that states that this seismicity is linked to low fracturing fluid recovery. For example, fracturing fluid recovery reported by Bao and

Eaton (2016) and Tan et al. (2020) shows that more than 90% and 50%, respectively, of the fracturing fluid remained in the subsurface in cases where earthquakes were believed to be triggered by fluid diffusion.

# CHAPTER 3

## METHODOLOGY

### 3.1 Model Description

The 2D numerical model is 20 km in width and 7.5 km in depth, and comprises of the shale formation, the hydraulically fractured “HF” region of the shale, and five layers of anisotropic hydraulic properties (see Figure 7). Permeable pathways intersecting the fractured region and/or the underlying layers are introduced to the model to assess the effect of the complexity of the network of interconnecting hydraulic conduits on the load recovery. Four horizontal wells are employed as part of the completion to account for the well interference that takes place during multi-lateral operations in real-life applications.

The simulation duration is composed of 2.5-days of injection, 5-days of shut-in period, and 90-days of production (Table 3). The initial conditions are taken to represent the pre-injection state of the formations.

**Table 3**

*The Stages of the Simulation*

Simulation stage	Duration	Description
Injection	2.5 days	Injecting fluid at 87.6 kg/m/s and 48 MPa
Shut-in	5 days	Wells are shut-in
Production	90 days	Producing fluids at 2.43 kg/m/s and 5 MPa

Figure 7 shows the location of the four horizontal wells that are assumed to be drilled in the shale layer and are illustrated with squares. It also displays the vertical permeability

values (in  $m^2$ ) of the different layers whereby the permeability distribution decreases with increasing depth (Pfund et al., 2016). To capture the heterogeneity of the layers, an anisotropy ratio for permeability is designated to the overburden region and the four underlying layers.

**Figure 7**

*Schematic of the 2D Model Showing the Permeability of the Layers and of the Hydraulic Conduit and the Four Horizontal Wells with Spacing of 600 m (Figure Not to Scale)*

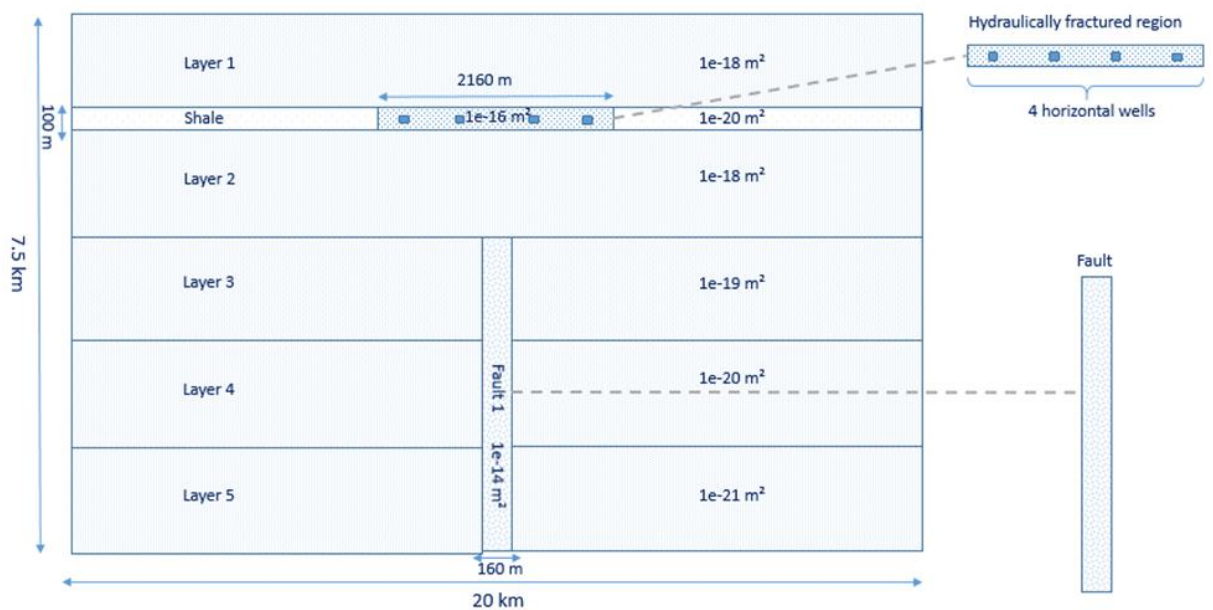


Figure 7 shows the vertical permeable pathway that intersects the layers and its permeability that is constant along the fault but has a higher value due to the presence of fault damage zones (Yehya et al., 2018). Although this assumption is conservative, the inclusion of such possible pathways is a common approach when studying fluid migration in the subsurface (Birdsell et al., 2015; Gassiat et al., 2013; Kissinger et al.,

2013; Lange et al., 2013; Myers, 2012; Pfunt et al., 2016; Reagan et al., 2015).

Furthermore, the hydraulically fractured region is modeled as a layer with enhanced permeability instead of explicitly representing the fractures because the work does not study the propagation of hydraulic fractures, but rather the effect of the complexity of the fracture network on fluid migration. Therefore, it is assumed that the hydraulic fractures extend to cover the thickness of the shale which generate a zone with enhanced permeability (Birdsell et al., 2015; Taherdangkoo et al., 2017). Two-phase flow representing the shale oil and the water (i.e. formation water and slick-water used in fracking operations) is considered.

Table 4 describes the input parameters used in the simulation. Source and sink terms, each of 4861 mol/m/s and 135 mol/m/s, respectively, are used in the simulation to monitor the injection and production of the contaminants dissolved in the fracturing fluid. A source/sink term is assigned to each of the four wells in the model, the values assigned to these terms allow them to act as inward fluxes during the injection period that fill the HF region with the fracturing fluid, and as outward fluxes during the production period that enable fracturing fluid removal out of the domain, of course while being shut-in during the shut-in period.

As for the maximum injected concentration referred to as " $C_{0_{max}}$ " in Table 4, it is the maximum concentration in the domain recorded at the source term in the HF region at the end of the injection period.  $C_{0_{max}}$  is obtained for a formation with no faults, and is used to normalize the reported recovery and concentration values in the results for all modeling scenarios.

**Table 4***Parameters Used in the Simulation*

Parameter	Value [unit]	Reference
Shale thickness	100 [m]	U.S. Energy Information Administration (U.S. EIA, 2020)
Shale porosity	0.01	Birdsell et al. (2015)
Shale permeability	1e-20 [m <sup>2</sup> ]	Liu et al. (2019)
Well spacing	600 [m]	He et al. (2020)
Overpressure gradient in shale	13 [kPa/m]	Gassiat et al. (2013) Birdsell et al. (2015)
Fracturing fluid density	1000 [kg/m <sup>3</sup> ]	Taherdangkoo et al. (2017)
Fracturing fluid viscosity	0.331 [mPa.s]	Pfunt et al. (2016)
Initial salinity	100 [kg/m <sup>3</sup> ]	Abbasi (2013)
Salinity gradient	0.11 [kg/m <sup>3</sup> /m]	Gassiat et al. (2013) Pfunt et al. (2016)
Freshwater density	1000 [kg/m <sup>3</sup> ]	(2013) Pfunt et al. (2016)
Water viscosity	0.8 [mPa.s]	Gassiat et al. (2013) Pfunt et al. (2016)
Irreducible water saturation in shale	0.2	Liu et al. (2019)
Bottom-hole flowing pressure	5 [MPa]	Liu et al. (2019)
Injection pressure	48 [MPa]	Wang et al. (2017)
		Liu et al. (2019)
		Ghanbari and Dehghanpour (2016)

Parameter	Value [unit]	Reference
Diffusivity coefficient	1e-9 [m <sup>2</sup> /s]	Taherdangkoo et al. (2017)
Inward mass flux (during injection)	87.6 [kg/m/s]	-
Outward mass flux (during production)	2.43 [kg/m/s]	-
Hydraulic fractures compressibility	1E-8 [1/Pa]	Liao et al. (2019)
Natural fractures compressibility	1.2E-7 [1/Pa]	Liu et al. (2019)
Gravity acceleration	9.8 [m/s <sup>2</sup> ]	-
Maximum injected concentration “ $C_{Omax}$ ”	1.2E+6 [mol/m <sup>3</sup> ]	-

### 3.2 Modeling Scenarios

We study four different scenarios while increasing the degree of network complexity as illustrated in Table 5 and Figure 8.

**Table 5**

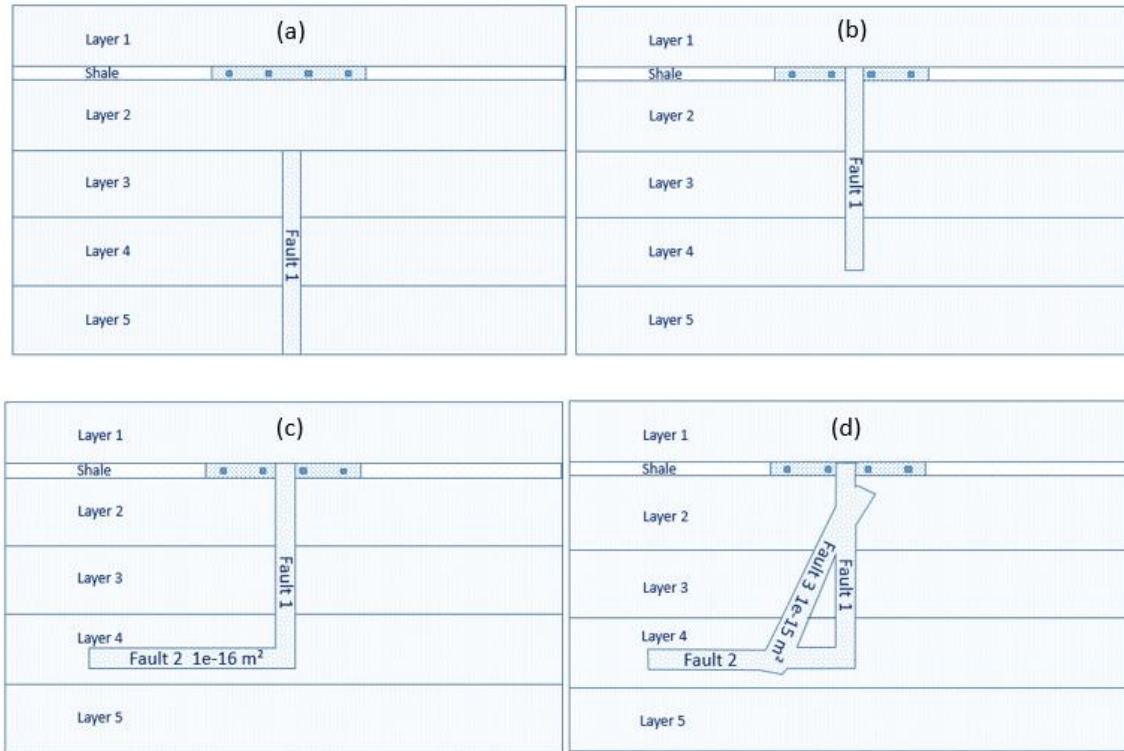
*Description of the Scenarios*

Name of scenario	Number of faults	Intersection with HF region	Degree of complexity <sup>1</sup>
Scenario 1 “SC 1”	1	✘	1
Scenario 2 “SC 2”	1	✓	2
Scenario 3 “SC 3”	2	✓	3
Scenario 4 “SC 4”	3	✓	4

<sup>1</sup> On a scale from 1 to 4, 1 being the least complex.

**Figure 8**

*Schematic Description of (a) Scenario 1 (SC1), (b) Scenario 2 (SC2), (c) Scenario 3 (SC3), and (d) Scenario 4*



### 3.3 Theory

#### 3.3.1 Mathematical Model

The model is a two-phase (water/oil), three-component fluid flow in porous media, in which the fracturing fluid constituents are conservative tracers in the water phase (adsorption and degradation effects are not accounted for). COMSOL Multiphysics finite element simulator was employed to implement the proposed model through coupling the Darcy's Law interface, with both the Phase Transport in Porous Media interface, and Transport of Diluted Species in Porous Media interface.

The mass conservation equation and Darcy's Law are given by,

$$\frac{\partial}{\partial t}(\epsilon_p \rho) + \nabla \cdot (\rho \mathbf{u}) = Q_m \quad (1)$$

$$\mathbf{u} = -\frac{k}{\mu}(\nabla p + \rho \mathbf{g}) \quad (2)$$

where,  $\mathbf{u}$  is the Darcy velocity,  $\epsilon_p$  is the porosity,  $k$  is the permeability,  $\rho$  is the density of the fluid,  $\mu$  is the viscosity of the fluid,  $p$  is the pressure,  $Q_m$  is a mass source, and  $\mathbf{g}$  is the gravitational acceleration.

To model the phase transport in porous media, the below equations are used:

$$\frac{\partial \epsilon_p \rho_{s_i} s_i}{\partial t} + \nabla \cdot \mathbf{N}_i = 0 \quad (3)$$

$$\mathbf{N}_i = \rho_{s_i} \mathbf{u}_i \quad (4)$$

$$\mathbf{u}_i = -\frac{k_{r_{s_i}}}{\mu_{s_i}} k \nabla p_{s_i} \quad (5)$$

where,  $s_i$  is saturation,  $\epsilon_p$  is the porosity,  $\rho_{s_i}$  is the density,  $k$  is the permeability of the porous medium,  $\mathbf{u}_i$  is the velocity,  $\mu_{s_i}$  is the dynamic viscosity,  $p_{s_i}$  is the pressure,  $\mathbf{N}_i$  is the fluid mass flux, and  $k_{r_{s_i}}$  is the relative permeability, and the subscript  $i$  indicates that the parameters are for phase  $i$ .

To model the transport of slick-water (HF fluid), we consider the transport of diluted species in porous media given as:

$$\frac{\partial[\epsilon_p c_i]}{\partial t} + \nabla \cdot \mathbf{J}_i + \mathbf{u} \cdot \nabla c_i = 0 \quad (6)$$

$$\mathbf{J}_i = -D_{e,i} \nabla c_i \quad (7)$$

$$D_{e,i} = \frac{\epsilon_p}{\tau_{F,i}} D_{F,i} \quad (8)$$

$$\tau_{F,i} = \epsilon_p^{-1/3} \quad (9)$$

where,  $c_i$  is the concentration of the chemical species,  $\mathbf{u}$  is the fluid velocity,  $\epsilon_p$  is the porosity,  $D_{e,i}$  is the effective diffusion,  $D_{F,i}$  is the diffusion coefficient, and  $\tau_{F,i}$  is the tortuosity.

### 3.3.2 Initial and Boundary Conditions

Initially, the pressure distribution of the domain is hydrostatic with an overpressure in the shale layer (Gassiat et al., 2013; Birdsell et al., 2015; Reagan et al., 2015; Taherdangkoo et al., 2017). The overburden and underlying regions, and permeable pathways are initially fully saturated with brine, while the fractured region is initially fully saturated with slick-water (Reagan et al., 2015; Ghanbari & Dehghanpour, 2016). The un-fractured shale is initially at irreducible water saturation (Liao et al., 2019). To differentiate between the slick-water and brine, the density of freshwater is assigned for the slick-water in the HF region, and a density that varies with depth is assigned for the brine to account for the variation of salinity as proposed by Pfunf et al. (2016) for the North German Basin.

The concentration of the fracturing fluid contaminants is initially zero for the entire domain and it is controlled by the source and sink terms throughout the simulation stages.

No-flux boundary conditions (Taherdangkoo et al., 2017) are selected for the four boundaries of the model by assuming a zero normal component of both the fluid mass and tracer fluxes as follows,

$$-\mathbf{n} \cdot \mathbf{N}_i = 0 \quad (10)$$

$$-\mathbf{n} \cdot (\mathbf{J}_i + \mathbf{u}c_i) = 0 \quad (11)$$

where,  $\mathbf{n}$  is the normal vector to the boundary,  $c_i$  is the concentration of the chemical species, and  $\mathbf{u}$  is the fluid velocity.

The size of the domain is chosen to be large enough so that the results are not affected by the boundaries. Accordingly, a sensitivity analysis of the domain size was performed to ensure no pressure perturbations reach the boundaries. Similarly, a sensitivity analysis on the mesh size was performed.

### ***3.3.3 Pressure-dependent Permeability***

Permeability in the subsurface can change due to mechanical deformation caused by stress changes and/or seismic damage (Yang et al., 2021), or chemical healing and sealing processes (Yehya et al., 2020). However, we focus here on the permeability changes caused by pressure increase and release during and after the hydraulic fracturing operations.

Following the opening of the hydraulic and natural fractures that occurs during the hydraulic fracturing operations, a pressure release takes place during the shut-in and production periods, which is expressed hydraulically by a decrease in pressure leading to the gradual closure of the fractures (Liao et al., 2019). This phenomenon should be included as it can affect the load recoveries, where a considerable fraction of the injected fracturing fluid is bound to be retained in the closing fractures as the pressure decreases. However, unlike the natural fractures, the permeability reduction of the hydraulic fractures after pressure release is constrained due to the presence of proppants. Hence, the pressure-dependent permeability change during the shut-in and production stages is governed by the following equation,

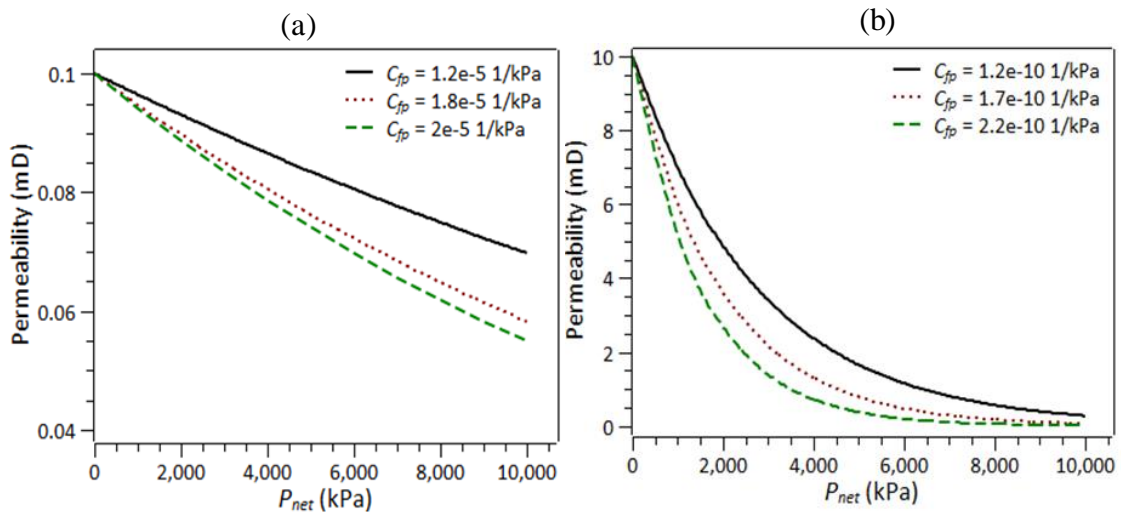
$$\frac{k}{k_0} = e^{3C_{fp}P_{net}} \quad (12)$$

where  $k$  is the permeability of the HF region and of the fault zone at any time step,  $k_0$  is the initial permeability,  $P_{net}$  is the net pressure within the fractures, and  $C_{fp}$  is the fracture compressibility.

Due to their different closure mechanisms, different compressibility values  $C_{fp}$  are assigned for propped (i.e., HF zone) and unpropped (i.e., fault zone) fractures. Figures 9a and 9b emphasize the sensitivity of the permeability to pressure changes, where permeability of the hydraulic fracturing zone and fault zone is calculated and plotted vs. the net pressure for different  $C_{fp}$  values. These plots show that the higher the compressibility of the fractures, regardless of their nature, the more sensitive the permeability is to the pressure changes and the faster they close. However, it remains evident that the presence of proppants in the hydraulic fractures highly restrains the permeability decline and prevents their complete closure or “locking”.

**Figure 9**

*Pressure-dependent Permeability During Shut-in and Production of the (a) Hydraulic Fracturing Zone, and (b) Fault Zone*



### 3.3.4 Recovery Calculation

The recovery of fracturing fluid is calculated from the concentration of fracturing fluid in the domain. The fracturing fluid is injected at the beginning of the injection period, where the concentration in the domain increases. During the shut in period, no fluid is injected and fracturing fluid diffuses within the domain. At the end of the shut-in period (i.e., the beginning of the production period) we measure the concentration  $C_i$  at every point in the domain. During the production period, the concentration of fracturing fluid in the domain decreases, as some fluid is produced by the well. We denote by  $C_e$  the concentration measured at every point in the domain at the end of the production period.

Hence, the recovery is calculated as

$$Recovery = \frac{\iint C_i - \iint C_e}{\iint C_{i_{max}}} \times 100 \quad (13)$$

where  $C_{i_{max}}$  is the maximum concentration recorded at the beginning of the production period among all the simulations run. The difference between the total fluid remaining in the domain between the first and last time step of production represents the fraction of the fluid that has been removed from the computational domain and hence produced by the well. The double integration over space provides us with a surface concentration value at each time step of the simulation. Moreover, in the results, we track the distribution of the fracturing fluid through normalized concentration profiles, which allow a better understanding of the migration of fracturing fluid within the domain.

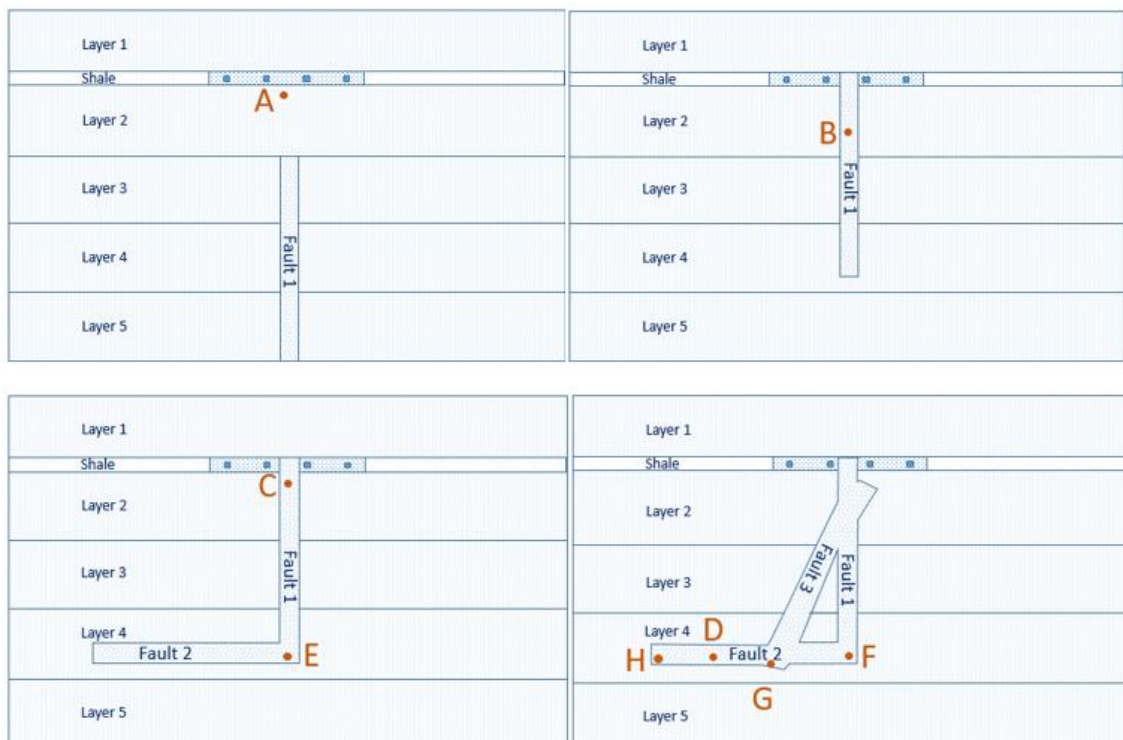
# CHAPTER 4

## RESULTS AND DISCUSSION

The results are reported by plotting the variation of the concentration of contaminants with time at chosen points within the domain for all models, and by calculating the load recovery using equation 13. The points are chosen carefully to best describe the migration of fluid within the domain and to identify the effects of faults and network complexity on the recovery. Figure 10 and Table A1 display the locations of the points for all scenarios.

**Figure 10**

*Locations of Points A-H*

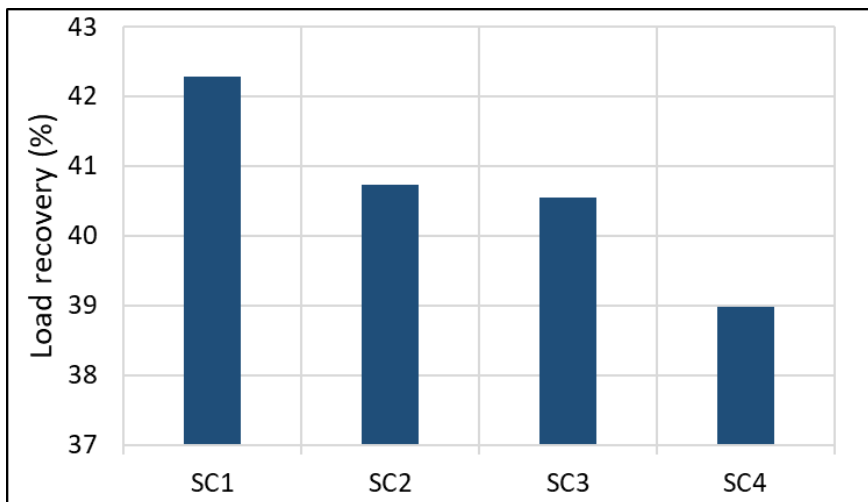


#### 4.1 Base case scenarios

The vertical bars in Figure 11 show the load recovery values for the four base case scenarios described in Figure 8 and Table 5. The only difference among these scenarios is the geometry of the fracture network and the degree of fracture complexity. Results show that the complexity and load recovery are negatively correlated; when the degree of complexity increases, the fluid recovery decreases. Hence, the more the hydraulic conduits are interconnected, the higher the volume of fluid that is entrapped in them, with limited the capability of flowing back to the surface.

**Figure 11**

*Recovery Values for the Base Case Scenarios*



#### 4.2 Parametric study

A parametric study on the base case models is used to assess the effect of several parameters on the recovery of the fracturing fluid. Table 6 shows the load recoveries calculated for the four scenarios when varying the shut-in and injection periods, faults' permeability, permeability of layers surrounding the HF region,

pressure-dependency of permeability, and the vertical distance between “fault 2” and the hydraulically fractured region.

**Table 6**

*Load Recovery Values Resulting from the Parametric Study*

Scenario	SC 1	SC 2	SC 3	SC 4
Base Case	42.3%	40.7%	40.5%	38.9%
Extending shut-in period from 5 days (base case) to 30 days	42.1%	40.5%	40.1%	38.4%
Extending injection period from 2.5 days (base case) to 5 days	42.4%	40.6%	40.4%	38.4%
Increasing permeability of layers 1 and 2 by a factor of $10^2$	41.1%	39.3%	37.9%	37.6%
Increasing permeability of layers 1 and 2 by a factor of $10^4$	42.7%	41.8%	42.2%	39.8%
Decreasing the permeability of fault 1 by a factor of $10^4$	41.2%	37.6%	39.5%	36.3%
Increasing the permeability of fault 2 by a factor of $10^4$			41.3%	40.9%
Decreasing the permeability of fault 2 by a factor of $10^2$			40.5%	38.9%
Increasing the permeability of fault 3 by a factor of $10^3$				40.5%
Decreasing the permeability of fault 3 by a factor of $10^3$				38.9%
Shortening the vertical distance between fault 2 and the hydraulically fractured region by 69%			41.1%	41.2%
Implementing a pressure-dependent permeability for the fault and fractures region	40.568%	39.363%	38.082%	36.328%

#### 4.2.1 *Effect of shut-in and injection periods*

Figure 12 compares the recovery obtained for the base case scenarios with cases with prolonged shut-in periods and prolonged injection periods. The shut-in period is increased from 5 days (base case) to 30 days while the injection period is increased

from 2.5 days (base case) to 5 days which correspond to typical ranges for injection and shut-in periods (see Table A2).

Figure 12 show that increasing the shut-in and injection periods both decrease the recovery for scenarios 2, 3 and 4, however, varying the injection period has a smaller effect on the recovery than the shut-in period for the number of days chosen in our models. For scenario 1, however, increasing the injection period yields a slight increase in the recovery. This different behavior could be attributed to the fact that SC 1 has the lowest network complexity and the fluid retention in fault 1 is not as substantial as in the other scenarios, hence, injecting a larger volume of fluid led to a higher recovery.

Moreover, monitoring the recovery values indicates that extending the shut-in period yield a larger decrease in the load recovery when the degree of network complexity rises (from SC1 through SC4); the decrease in the recovery from the base case is 0.47%, 0.49%, 0.98%, and 1.3% for SC1, SC2, SC3, and SC 4 respectively.

**Figure 12**

*Recovery Values for Different Shut-in and Injection Periods*

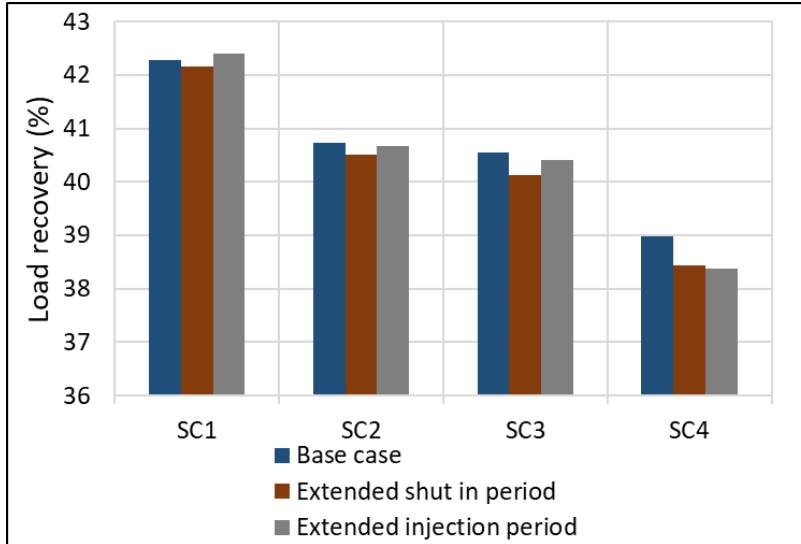
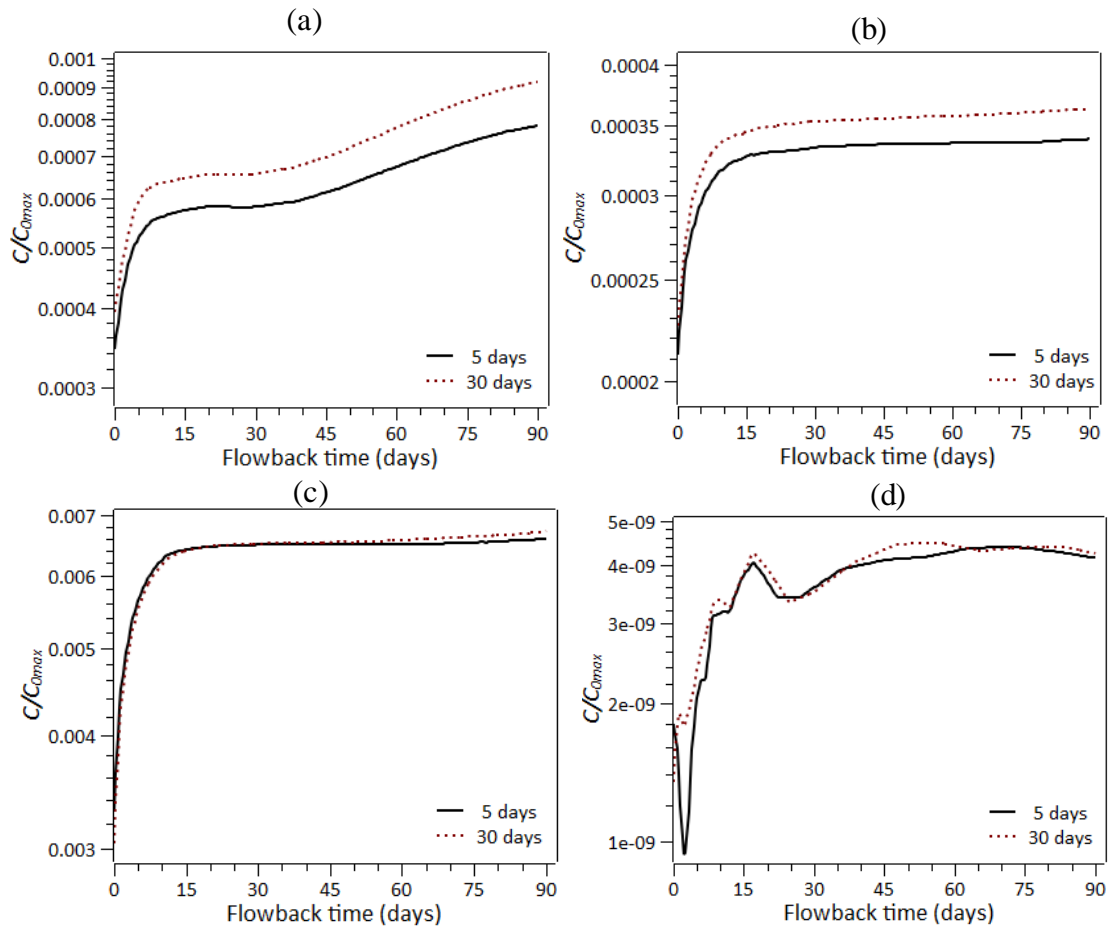


Figure 13 shows the concentration of the fracturing fluid within the formation for the four scenarios at different shut-in periods and as a function of production/flow-back time. The values are reported in terms of normalized concentration  $C/C_{0max}$ , where  $C$  is the concentration of the fracturing fluid in  $\text{mol/m}^3$  at the defined point and  $C_{0max}$  is the maximum in  $\text{mol/m}^3$  (defined in section 3.1).

For all scenarios, the normalized concentration remaining in the domain, as production proceeds, is higher for longer shut-in periods. This explains the lower recovery values obtained (see Figure 12), because longer shut-in gives the fracturing fluid more time to diffuse into the surrounding layers and into the hydraulic conduits. Hence, the available surface area for water imbibition is larger, and larger percentage of this fluid remains in the subsurface and in the faults' network, which inhibits the recovery of the fracturing fluid from the wells.

**Figure 13**

*Normalized Concentration Change vs. Flow-Back Time for 5 and 30 Days of Shut-In Period Measured (a) at Point A in SC1, (b) at Point B in SC2, (b) at Point C in SC3, and (d) at Point D in SC4. Points A-D are Shown in Figure 10*



#### 4.2.2 Effect of subsurface permeability structure

We examine the effect of the permeability of the two layers surrounding the HF zone (i.e., layers 1 and 2) and of the permeable pathways (i.e., faults 1, 2, and 3).

Figures 14 and 15 compare the load recoveries for the base cases of the four scenarios

with cases where we increase the permeability of the two confining layers, and of faults 2 and 3. Table 7 describes the values of the permeability.

**Figure 14**

*Recovery Values for the Base Case and for Increased Permeability of Layers 1 and 2*

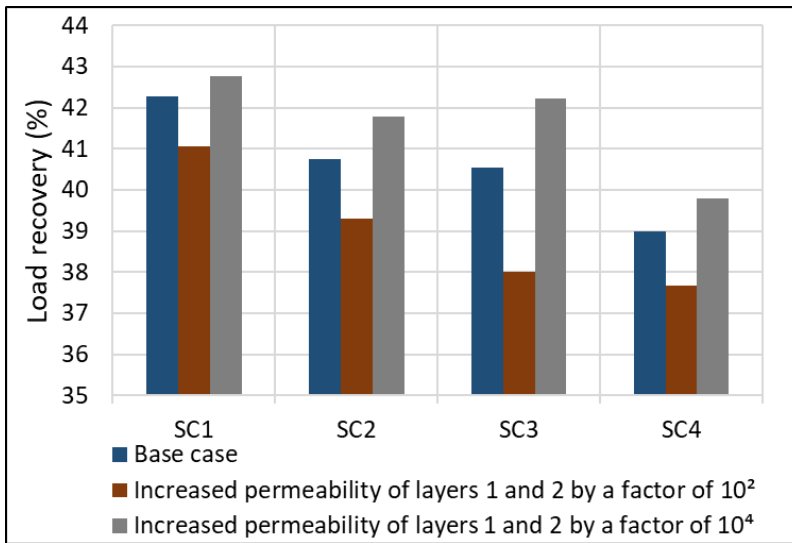
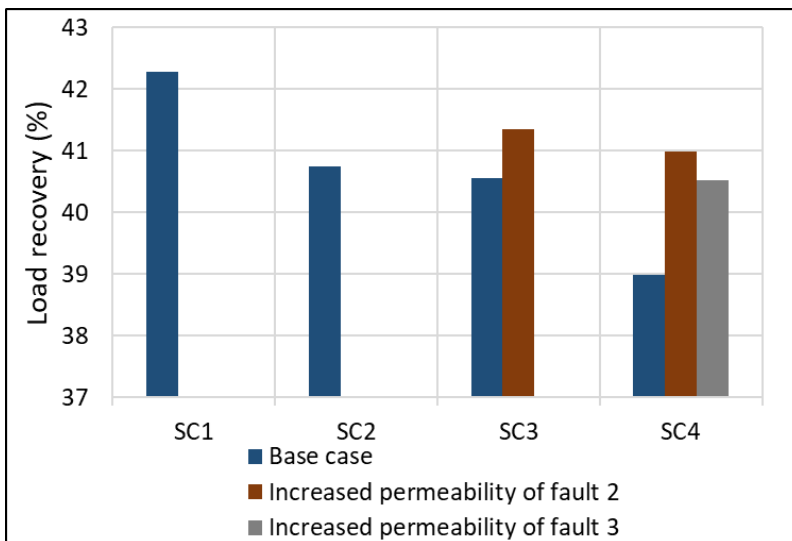


**Figure 15**

*Recovery Values for the Base Case and for Increased Permeability of Faults 2 and 3*



The bar diagrams indicate that increasing the permeability of the faults leads to a rise in the recovery (see Figure 15). However, the relation between the permeability of the layers surrounding the HF zone and the load recovery is more complex. Increasing the permeability of the surrounding layers to  $1\text{e-}16\text{ m}^2$  leads to a drop in the recovery, while increasing the permeability to  $1\text{e-}14\text{ m}^2$  leads to a gain in the recovery compared to base case scenarios.

**Table 7**

*Permeability Values of Layers 1 & 2, Fault 2, and Fault 3 for Different Cases*

Formation/ Fault	Base case permeability	Increased permeability	
Layers 1 and 2	$1\text{e-}18\text{ m}^2$	$1\text{e-}14\text{ m}^2$	$1\text{e-}16\text{ m}^2$
Fault 2	$1\text{e-}16\text{ m}^2$	$1\text{e-}12\text{ m}^2$	
Fault 3	$1\text{e-}15\text{ m}^2$	$1\text{e-}12\text{ m}^2$	

Keeping in mind that the permeability of the hydraulically fractured region in all cases is  $1\text{e-}16\text{ m}^2$  (and that of the shale is  $1\text{e-}20\text{ m}^2$ ), we note from the results that if the permeability of the formations/structures surrounding or intersecting the HF region is higher than that of the HF region (i.e.,  $1\text{e-}16\text{ m}^2$ ) the fracturing fluid recovery increases. However, if the permeability of the formations/structures surrounding or intersecting the HF region is lower, then the flow-back decreases.

Hence, the reduction in recovery noticed when the permeability of the surrounding layers 1 and 2 was increased to  $1\text{e-}16\text{ m}^2$  (equaling that of the HF region), and the increase in recovery when the permeability was increased to  $1\text{e-}14\text{ m}^2$  (which is higher than that of the HF region) is explained as follows. When the permeability of the surrounding layers is lower than that of the HF region (i.e. base case scenario), a

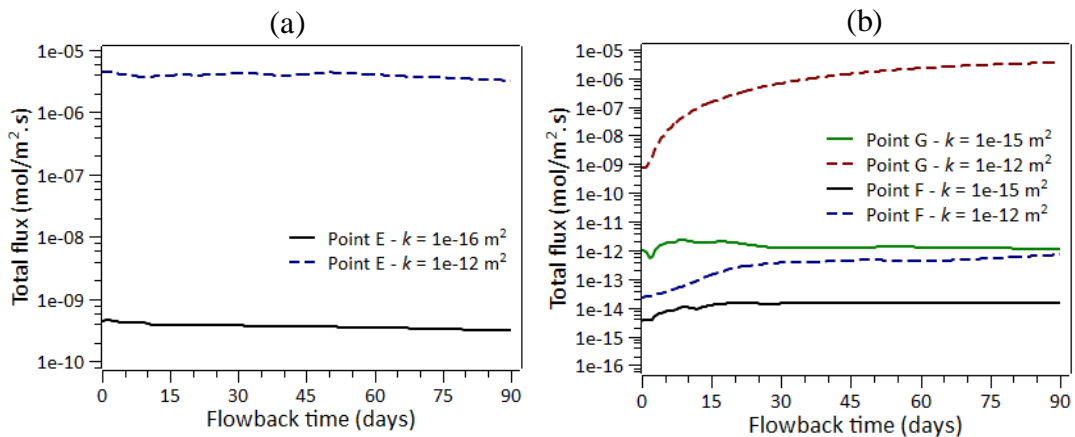
fraction of the fracturing fluid that imbibes into the surrounding formation is not entirely produced back by the wells during the 90-day period, because the reduced permeability values restrict the fluid flow. When the permeability of the surrounding layers is increased to values equal or lower than that of the HF region, a larger fraction of the fluid imbibes into the formation because the fluid's diffusion into the formation is facilitated. However, since the formations' permeability is still not higher than that of the HF region, the larger quantity of stored fluid is not able to be produced back. Accordingly, in the base case scenarios the volume of fluid stored is limited by the poorer permeability values that do not allow easy fluid seepage. An increase in the permeability of the surrounding layers is not large enough to allow the volume of fluid that is retained in the formation to be produced at a rate higher than the base case scenarios hence, lower recovery values. On the other hand, although the additional increase in the surrounding layers' permeability to values higher than that of the HF region might further promote fluid diffusion, the flowback in this case is facilitated enough to restrain the consequences of this diffusion and it leads to the higher recovery reported.

The recovery increases with higher fault permeability because the permeability of the fault is assumed to be higher than that of the HF zone. Hence, the HF fluid can migrate back to the well during the production period. This is verified in Figure 16 that shows the total flux versus flow-back time for SC 3 for different permeability values of fault 2, and for SC 4 for different permeability values of fault 3. Based on the trends of Figure 16, and noting that the points where the fluxes are recorded are at the intersections of the faults (i.e. point E at the intersection of faults 1 and 2, point F at the intersection of faults 1 and 2, and point G at the intersection of faults 2 and 3), we can

see that the flux is higher when the permeability is enhanced, and this is because the increased permeability facilitates the fluid flow back towards the producing wells which translates into the higher load recovery reported earlier in Table 6.

**Figure 16**

*Total Flux vs. Flow-back Time Measured (a) at Point E in SC3 for Different Permeability Values of Fault 2, and (b) at Points F and G in SC4 for Different Permeability Values of Fault 3. Figure 10 Shows the Locations of Points E, F, and G*



#### 4.2.3 Effect of temporal evolution of permeability

As illustrated previously, permeability changes driven by pressure variations have a considerable impact on the flow-back process of the fluid and hence on the total recovery. Figure 17 displays the change in permeability of the hydraulically fractured region, and of faults 1, 2 and 3 in SC 4. The permeability values indicate that the sensitivity of the hydraulic fractures to pressure variations is lower than that of the faults and this is due to the proppants filling the fractures.

**Figure 17**

*Permeability of the HF Region, Fault 1, Fault 2, and Fault 3 as a Function of Post Injection Time for SC4 when Assuming a Pressure -dependent Permeability Model*

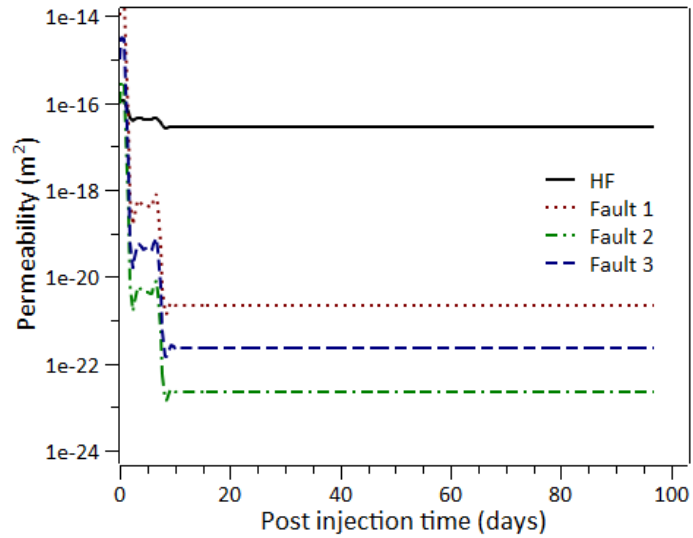


Figure 18 compares the recovery values for the base case scenarios against the cases with pressure-dependent permeability (i.e. permeability variation of both the HF and faults' regions in the four scenarios) and indicates that accounting for permeability variations leads to lower load recovery. Surprisingly, this phenomenon is commonly ignored even though it has a significant effect on the recovery of fracturing fluid. Fluids diffuse faster when the permeability is high during high-pressure injection, and then the permeability drops due to pressure dissipation, which leads portion of the fluids to be trapped in the subsurface.

**Figure 18**

*Recovery Values for the Base Case Scenarios and the Formation with Pressure-dependent Permeability*

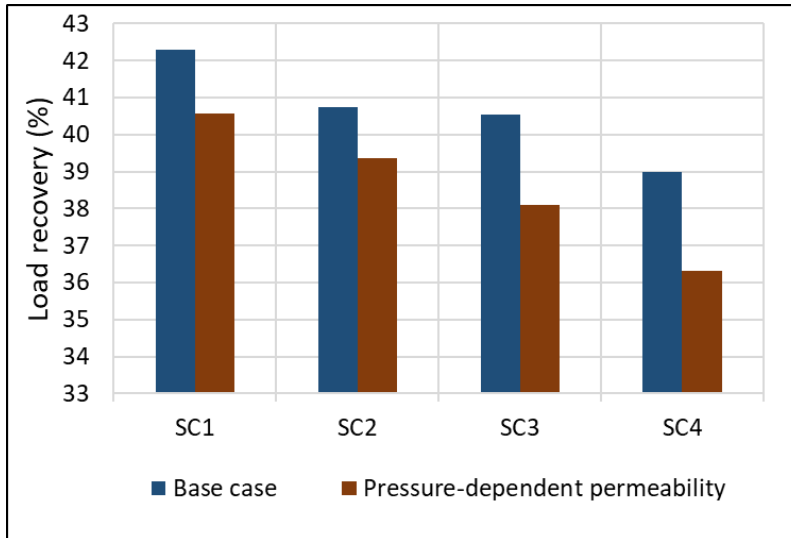
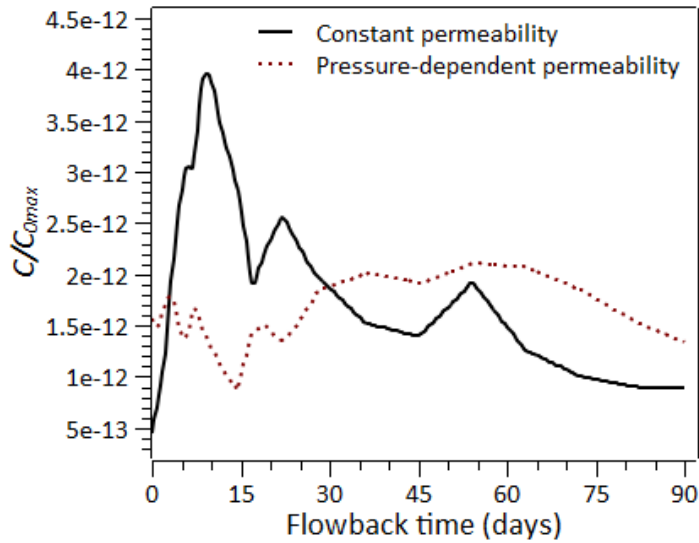


Figure 19 compares the normalized concentration curves for the base case of SC4 (i.e., where permeability is kept constant) and the case where permeability varies with pressure. The concentration measured at the designated points in the model is higher for formations with pressure-dependent permeability which confirms that when the fractures close, more fluid gets entrapped in them, and the fluid is unable to be produced by the well which leads to a lower load recovery.

**Figure 19**

*Normalized Concentration Change in SC4 at Point H (Shown in Figure 10) vs Flow-back Time for a Formation with Constant Permeability and a Pressure-dependent Permeability*



### 4.3 Discussion

#### 4.3.1 Limitations

During the flow-back phase, the produced water collected at the surface is a mixture of both the formation water (i.e. brine) and the re-produced fracturing fluid. This makes the accurate calculation of fracturing fluid recovery a challenging task, where detailed chemical and isotropic tracing approaches are required to differentiate between the produced brine and the recovered fracturing fluid.

Moreover, recovery calculation in our work is further complicated due to the fact that COMSOL provides the saturation profiles and flow rates of water and oil without differentiating between slick-water and brine. So, we resort to calculating the recovery

using equation 13, based on the concentration of contaminants dissolved in the fracturing fluid rather than the fluid volumes and water flow rates.

Another limitation in this work is the assumption that there are no gravity effects in the vicinity of the wellbore. Gravity forces along the lateral section of the horizontal wells might lead to fluid settlement in this section, where high pressure drawdown is required along the lateral part to make the fluid mobile, thus contributing to the incomplete return of the fracturing fluid. However, our 2D model does not support simulating the lateral section of the well.

Consequently, due to these limitations this study is considered a parameter-dependent one with conclusions being derived based on the chosen parameters.

#### ***4.3.2 Implications on the safety of nearby aquifers***

Findings presented in this paper give insights about the transport of the fracturing fluid in the subsurface, and the possible causes of the low recovery. As a result, such findings shed the light on the importance of estimating the time needed for fluid migration in the subsurface as it has direct implications on the contamination of drinking water aquifers. Even though, when faults are absent, the migration of HF is slow and the water contamination would only happen after a “long period”, the difficulty resides in defining long periods for sustainable practices.

The time  $t$  needed for fluid to migrate is approximated by assuming that the microcracks and pore space in the subsurface region between the trapped fluid and the aquifer are tortuous channel with an average radius  $R$  and inclination  $\theta$ , hence  $t$  is given by

$$t = \frac{16\lambda\mu x}{R^2(\bar{p} - \rho g \sin\theta)} \quad (14)$$

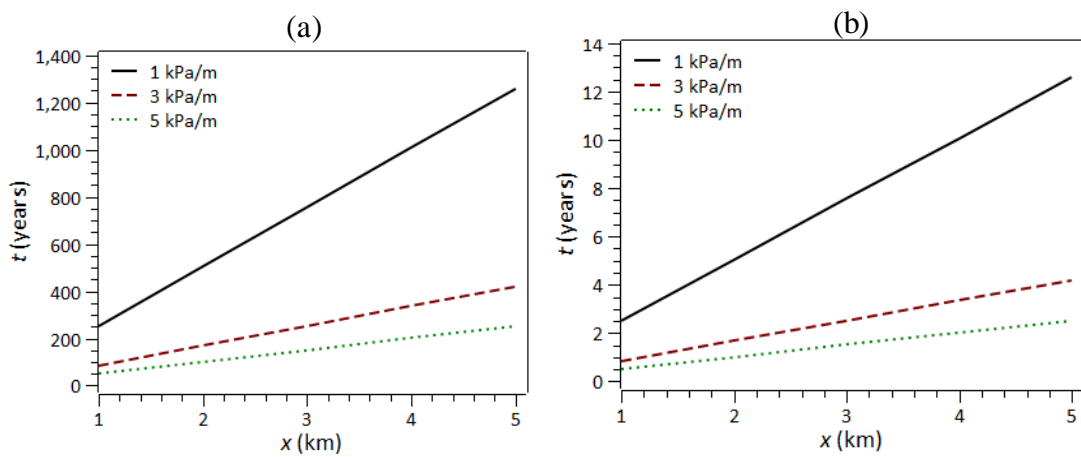
where  $x$  is the distance between the current location of the fluid and the aquifer,  $\lambda$  (assumed equal to 150) is a correction factor to account for the tortuosity of the channels,  $\mu$  is the dynamic viscosity of the fluid,  $\rho$  is the fluid density,  $g$  is the magnitude of gravitational acceleration, and  $\bar{p}$  is the driving pressure per linear meter (expressed in MPa/m). If  $\theta$  is zero, then there is no effect of gravity on the migration of fluid and the fluid can start migrating to the aquifer even for a very low driving pressure value. If  $\theta$  is non-zero, the driving pressure per linear meter should be greater than  $\rho g \sin\theta$  for the fluid to infiltrate to the aquifer. When  $\theta=90^\circ$ ,  $\bar{p}$  should exceed 9.8 kPa/m for the fracking fluid to start migrating to the aquifer. The required pressure gradient decreases as  $\theta$  decreases. This threshold can be reached near shale reservoirs as some site studies showed an overpressure of an average of 15kPa/m (Eaton & Schultz, 2018). The time  $t$  linearly increases with the distance to the aquifer when all other parameters are fixed. It decreases as the net driving pressure per linear meter ( $\bar{p} - \rho g \sin\theta$ ) and  $R$  increase.

Plots in Figure 20 show the time in years calculated as a function of the distance between the fluid and the aquifer, for different values of the net driving pressure per linear meter ( $\bar{p} - \rho g \sin\theta$ ). We choose values of  $R$  of 10 micrometers, which gives an average permeability  $k_{avg}$ , (Figure 20 a) and 100 micrometers, which gives an equivalent permeability of  $100 k_{avg}$ , (Figure 20 b). Increasing  $R$  by a ratio of 10, results roughly in an increase by 100 in the average permeability ( $k_{avg}$ ). From the results, we deduce that it takes the fluid longer time to reach the aquifer in any of the following cases: smaller radius (lower average permeability), longer distance, or lower net driving pressure per linear meter. Comparing the time calculated in both graphs shows that increasing  $R$  by a factor of 10 decreases the migration time by a factor of 100.

Lastly, it should be pointed out that the time scale spans over a wide range that varies from a couple of years up to thousands of years. The variability in time highlights the importance of assessing the long-term effects of the hydraulic fracturing practices and not neglecting them, because the environmental hazard caused by the fluids might require several years to be noticed or detected.

**Figure 20**

*Time Needed for the Fluid to Migrate vs. the Distance Between the Fluid and the Aquifer for Different Values of Net Driving Pressure Per Linear Meter and for Permeability (a)  $k_{avg}$ , and (b)  $100k_{avg}$*



## CHAPTER 5

### CONCLUSION

In this work, we discuss the environmental impact of the fracturing fluid and the risks associated with its usage and its migration into drinking water sources. We also provide new insights on the fate of the fracturing fluid and the low recovery values noted in the industry through evaluating the effect of various parameters on the fluid recovery. We use numerical models of two-phase flow of oil and water during and after the hydraulic fracturing of a shale formation with pre-existing fault network. First, four base case scenarios are analyzed with different geometries of the interconnected faults. Then, the impact of the shut-in period, injection period, faults' permeability, surrounding layers' permeability, and pressure-dependent permeability is analyzed whereby the fluid recovery and the fracturing fluid concentration are calculated.

The simulation results demonstrate a negative correlation between the fracture network complexity represented by the interconnecting faults and the recovery of the fracturing fluid. The more complex the network, the more the fluid is retained in the formation. The same applies to extending the shut-in period, where the volume of fluid retained increases resulting in a lower fracturing fluid recovery. For all simulated scenarios, recovery increases when permeability of the formations/structures surrounding or intersecting the HF region exceeds that of the HF region. Enhancement of the permeability of the subsurface structure develops an easier path for the fluid to flow through, thus deriving a higher recovery. Furthermore, the models show the importance of implementing a pressure-dependent permeability of fractures and faults as it decreases fluid recovery and can explain the

reported low recovery data in most study cases. The permeability decreases during production due to the decrease in formation pressure and the closure of the hydraulic/natural fractures, and the fluid that was injected into the fractures is most likely to remain there regardless of the suction power.

Finally, the time needed for trapped fracking fluid to migrate to nearby aquifers ranges from a few months to hundreds of years. Consequently, it is crucial to assess the long-term effects of the hydraulic fracturing practices because the associated environmental hazards might require several years to be noticed or detected.

## APPENDIX

**Table A1**

*Coordinates and names of Points Used for Measuring Concentration and Flux*

Point name	Coordinates	
	x (m)	y (m)
A	10570	4500
B	10570	4000
C	10570	4750
D	8490	1530
E	10570	1610
F	10564	1540
G	9610	1465
H	7280	1530

**Table A2**

*Typical Injection, Shut-in, and Simulation Durations in the Literature*

Injection duration [unit]	Shut-in duration [unit]	Simulation duration [unit]	Reference
2 [hours]	5 [days]	10 [days]	Liu et al. (2019)
1 [hour]	1 [day]	3 [months]	Zanganeh et al. (2015)
2.5 [days]	5 [days]	20 [years]	Birdsell et al. (2015)
2 [hours]	22 [hours]	6 [months]	Liao et al. (2019)
2.5 [days]	5 [days]	30 [years]	Taherdangkoo et al. (2019)
1.5 [hours]	24 [hours]	25.5 [hours]	Wang et al. (2017)
10 [days]	90 [days]	20 [years]	Almulhim (2014)
24 [hours]	N/A	800 [days]	Nabizadeh et al. (2016)
3.5 [hours]	N/A	300 [years]	Pfunt et al. (2016)

## REFERENCES

- Abaa, K., Wang, J.Y. & Ityokumbul, M.T. (2013). Parametric study of fracture treatment parameters for ultra-tight gas reservoirs. *Journal of Petroleum Exploration and Production Technology*, 3, 159–168.  
<https://doi.org/10.1007/s13202-013-0058-x>
- Abbassi, M. A. (2013). *A Comparative Study of Flowback Rate and Pressure Transient Behaviour in Multifractured Horizontal Wells* [Master's Thesis, University of Alberta]. Education and Research Archive.  
<https://era.library.ualberta.ca/items/729fe8b4-12c1-4984-9209-c9a615e98530>
- Abdulelah, H., Mahmood, S. M., Al-Hajri, S., Hakimi, M., & Padmanabhan, E. (2018). Retention of Hydraulic Fracturing Water in Shale: The Influence of Anionic Surfactant. *Energies*, 11 (12). <https://doi.org/10.3390/en1123342>
- Almulhim, A. (2014). *Fluid Flow Modeling in Multi-Stage Hydraulic Fracturing Patterns for Production Optimization in Shale Reservoirs* [Master's Thesis, Colorado School of Mines]. Mines Repository.  
<http://hdl.handle.net/11124/12276>
- Arthur, J. D., Bohm, B., Coughlin, B., & Layne, M. (2008). *Hydraulic Fracturing Considerations for Natural Gas Wells of the Fayetteville Shale*.
- Aseperi, T. C. (2015, May). *Numerical Modeling of Fluid Migration in Hydraulically Fractured Formations* [Doctoral Thesis, University of Arkansas, Fayetteville]. ScholarWorks@UARK. <http://scholarworks.uark.edu/etd/1095>

- Bao, X., & Eaton, D.W. (2016). Fault activation by hydraulic fracturing in western Canada. *Science*, 354(6318), 1406-1409.  
<https://doi.org/10.1126/science.aag2583>
- Birdsell, D. T., Rajaram, H., Dempsey, D., & Viswanathan, H.S. (2015). Hydraulic fracturing fluid migration in the subsurface: A review and expanded modeling results. *Water Resources Research*, 51, 7159–7188.  
<https://doi.org/10.1002/2015WR017810>
- Birkle, P. (2016). Recovery rates of fracturing fluids and provenance of produced water from hydraulic fracturing of Silurian Qusaiba hot shale, northern Saudi Arabia, with implications on fracture network. *AAPG Bulletin*, 100(6), 917-941.  
<https://doi.org/10.1306/02101615120>
- DiGiulio, D.C., & Jackson, R.B. (2016). Impact to Underground Sources of Drinking Water and Domestic Wells from Production Well Stimulation and Completion Practices in the Pavillion, Wyoming, Field. *Environmental Science & Technology*, 50(8), 4524-4536. <https://doi.org/10.1021/acs.est.5b04970>
- Eaton, D. W., & Schultz, R. (2018). Increased likelihood of induced seismicity in highly overpressured shale formations. *Geophysical Journal International*, 214(1), 751-757. <https://doi.org/10.1093/gji/ggy167>
- Elliot, E.G., Ettinger, A.S., Leaderer, B.P., Bracken, M.B., & Deziel, N.C. (2016). A systematic evaluation of chemicals in hydraulic-fracturing fluids and wastewater for reproductive and developmental toxicity. *Journal of Exposure Science & Environmental Epidemiology*, 27, 90-99. <https://doi.org/10.1038/jes.2015.81>

- Fakcharoenphol, P., Torcuk, M., Bertoncello, A., Kazemi, H., Wu, Y., Wallace, J., & Honarpour, M. (2013, September 30 - October 2). *Managing Shut-in Time to Enhance Gas Flow Rate in Hydraulic Fractured Shale Reservoirs: A Simulation Study* [Paper presentation]. SPE Annual Technical Conference and Exhibition, New Orleans, Louisiana, USA. <https://doi.org/10.2118/166098-MS>
- Fan, L., J. W. Thompson, & J. R. Robinson (2010, October 19-21). *Understanding gas production mechanism and effectiveness of well stimulation in the Haynesville Shale through reservoir simulation* [Paper presentation]. Canadian Unconventional Resources and International Petroleum Conference, Alberta, Canada. <https://doi.org/10.2118/163980-MS>
- Figueiredo, B., Tsang, C. F., Rutqvist, J., & Niemi, A. (2017). Study of hydraulic fracturing processes in shale formations with complex geological settings. *Journal of Petroleum Science and Engineering*, 152, 361–374. <https://doi.org/10.1016/j.petrol.2017.03.011>
- Fu, Y., & Dehghanpour, H. (2020). How far can hydraulic fractures go? A comparative analysis of water flowback, tracer, and microseismic data from the Horn River Basin. *Marine and Petroleum Geology*, 115. <https://doi.org/10.1016/j.marpetgeo.2020.104259>
- Gassiat, C., Gleeson, T., Lefebvre, R., & McKenzie, J. (2013). Hydraulic fracturing in faulted sedimentary basins: Numerical simulation of potential contamination of shallow aquifers over long time scales. *Water Resources Research*, 49 (12), 8310-8327. <https://doi.org/10.1002/2013WR014287>

- Ghanbari, E., & Dehghanpour, H. (2016). The fate of fracturing water: A field and simulation study. *Fuel*, 163, 282–294. <https://doi.org/10.1016/j.fuel.2015.09.040>
- He, Y., Guo, J., Tang, Y., Xu, J., Li, Y., Wang, Y., Lu, Q., Patil, S., Rui, Z., & Sepehrnoori, K. (2020, October 26-29). *Interwell Fracturing Interference Evaluation of Multi-Well Pads in Shale Gas Reservoirs: A Case Study in WY Basin* [Paper presentation]. SPE Annual Technical Conference & Exhibition, Denver, Colorado, USA. <https://doi.org/10.2118/201694-MS>
- Henderson, C., Matis, H., Kommepalli, H., Moore, B., Wang, H., & Acharya, H. (2011). *Cost Effective Recovery of Low-TDS Frac Flowback Water for Re-use*. Office of Scientific and Technical Information. <https://www.osti.gov/servlets/purl/1030557>
- Hirono, T., Takahashi, M., & Nakashima, S. (2003). In situ visualization of fluid flow image within deformed rock by X-ray CT. *Engineering Geology*, 70 (1-2), 37-46. [https://doi.org/10.1016/S0013-7952\(03\)00074-7](https://doi.org/10.1016/S0013-7952(03)00074-7)
- Hsu, S.M., Ke, C.C., Dong, M.C., & Lin, Y.T. (2022). Investigating fault zone hydraulic properties and groundwater potential in a fault-dominated aquifer system: A case study of the Dili fault in Central Taiwan. *Engineering Geology*, 308. <https://doi.org/10.1016/j.enggeo.2022.106805>
- Hui, G., Chen, S., Gu, F., Wang, H., Zhang, L., & Yu, X. (2021). Influence of hydrological communication between basement-rooted faults and hydraulic fractures on induced seismicity: A case study. *Journal of Petroleum Science and Engineering*, 206. <https://doi.org/10.1016/j.petrol.2021.109040>

- Ingraffea, A.R., Wells, M.T., Santoro, R.L., & Shonkoff, S.C. (2014). Assessment and risk analysis of casing and cement impairment in oil and gas wells in Pennsylvania, 2000–2012. *Proceedings of the National Academy of Sciences*. <https://doi.org/10.1073/pnas.1323422111>
- Ishii, E. (2017). Preliminary assessment of the highest potential transmissivity of fractures in fault zones by core logging. *Engineering Geology*, 221, 124-132. <https://doi.org/10.1016/j.enggeo.2017.02.026>
- Jia, H., McLennan, J., & Deo, M. (2013). The Fate of Injected Water in Shale Formations. In A. P. Bungler, J. McLennan, & R. Jeffrey (Eds.), *Effective and Sustainable Hydraulic Fracturing*. IntechOpen. <https://doi.org/10.5772/56443>
- Karimi, S., Baturan, D., & Yenier, E. (2018). Five key lessons gained from induced seismicity monitoring in western Canada. *The Leading Edge*, 37(2). <https://doi.org/10.1190/tle37020107a1.1>
- Khadijeh, M., Yehya, A., & Maalouf, E. (2022). Propagation and geometry of multi-stage hydraulic fractures in anisotropic shales. *Geomechanics and Geophysics for Geo-Energy and Geo-Resources*, 8(4), 1-24.
- Khan, H. J., Eleanor, S., Jew, A. D., Bargar, J., Kovscek, A., & Druhan, J. L. (2021). A Critical Review of the Physicochemical Impacts of Water Chemistry on Shale in Hydraulic Fracturing Systems. *Environmental Science & Technology*, 55 (3), 1377-1394. <https://dx.doi.org/10.1021/acs.est.0c04901>
- Khang, N.D., Watanabe, K., & Saegusa, H. (2004). Fracture step structure: geometrical characterization and effects on fluid flow and breakthrough curve. *Engineering Geology*, 75(1), 107-127. <https://doi.org/10.1016/j.enggeo.2004.05.004>

- King, G. E. (2012, February 6-8). *Hydraulic Fracturing 101: What Every Representative, Environmentalist, Regulator, Reporter, Investor, University Researcher, Neighbor and Engineer Should Know About Estimating Frac Risk and Improving Frac Performance in Unconventional Gas and Oil Wells* [Paper presentation]. SPE Hydraulic Fracturing Technology Conference, The Woodlands, Texas, USA. <https://doi.org/10.2118/152596-ms>
- Kissinger, A., Helmig, R., Ebigbo, A., Class, H., Lange, T., Sauter, M., Heitfeld, M., Klünker, J., & Jahnke, W. (2013). Hydraulic fracturing in unconventional gas reservoirs: risks in the geological system, part 2. *Environmental Earth Sciences*, 70(8), 3855–3873. <https://doi.org/10.1007/s12665-013-2578-6>
- Kreipl, M.P., & Kreipl, A.T. (2017). Hydraulic fracturing fluids and their environmental impact: then, today, and tomorrow. *Environmental Earth Sciences*, 76. <https://doi.org/10.1007/s12665-017-6480-5>
- Lange, T., Sauter, M., Heitfeld, M., Schetelig, K., Brosig, K., Jahnke, W., Kissinger, A., Helmig, R., Ebigbo, A., & Class, H. (2013). Hydraulic fracturing in unconventional gas reservoirs: risks in the geological system part 1. *Environmental Earth Sciences*, 70(8), 3839–3853. <https://doi.org/10.1007/s12665-013-2803-3>
- Li, G., Li, G., Wang, Y., Qi, S., & Yang, J. (2020). A rock physics model for estimating elastic properties of upper Ordovician lower Silurian mudrocks in the Sichuan Basin, China. *Engineering Geology*, 266. <https://doi.org/10.1016/j.enggeo.2019.105460>

- Li, L. C., Tang, C. A. A., Li, G., Wang, S. Y., Liang, Z. Z., & Zhang, Y. B. (2012). Numerical Simulation of 3D Hydraulic Fracturing Based on an Improved Flow-Stress-Damage Model and a Parallel FEM Technique. *Rock Mechanics and Rock Engineering*, 45, 801–818. <https://doi.org/10.1007/s00603-012-0252-z>
- Li, Y., Guo, J., Zhao, J., & Yue, Y. (2007). A New Model of Fluid Leak-off in Naturally Fractured Gas Fields and Its Effects on Fracture Geometry. *Journal of Canadian Petroleum Technology*, 46(12). <https://doi.org/10.2118/07-12-tn1>
- Liao, K., Zhang, S., Ma, X., & Zou, Y. (2019). Numerical Investigation of Fracture Compressibility and Uncertainty on Water-Loss and Production Performance in Tight Oil Reservoirs. *Energies*, 12(7), 1189. <https://doi.org/10.3390/en12071189>
- Liu, D., Li, J., Zou, C., Cui, H., Ni, Y., Liu, J., Wu, W., Zhang, L., Coyte, R., Kondash, A., & Vengosh A. (2020). Recycling flowback water for hydraulic fracturing in Sichuan Basin, China: Implications for gas production, water footprint, and water quality of regenerated flowback water. *Fuel*, 272. <https://doi.org/10.1016/j.fuel.2020.117621>
- Liu, H., Hu, X., Guo, Y., Ma, X., Wang, F., & Chen, Q. (2019). Fracture Characterization Using Flowback Water Transients from Hydraulically Fractured Shale Gas Wells. *ACS Omega*, 4 (12), 14688-14698. <https://doi.org/10.1021/acsomega.9b01117>
- Llewellyn, G. T., Dorman, F., Westland, J. L., Yoxtheimer, D., Grieve, P., Sowers, T., Humston-Fulmer, E., & Brantley, S. L. (2015). Evaluating a groundwater supply contamination incident attributed to Marcellus Shale gas development.

*Proceedings of the National Academy of Sciences*, 112(20), 6325–6330.

<https://doi.org/10.1073/pnas.1420279112>

McClure, M. (2014, April 1-3). *The Potential Effect of Network Complexity on Recovery of Injected Fluid Following Hydraulic Fracturing* [Paper presentation]. SPE Unconventional Resources Conference, The Woodlands, Texas, USA. <https://doi.org/10.2118/168991-ms>

Mrdjen, I., & Lee, J. (2015). High volume hydraulic fracturing operations: potential impacts on surface water and human health. *International Journal of Environmental Health Research*, 26(4), 361-380.

<http://dx.doi.org/10.1080/09603123.2015.1111314>

Murphy, R.P. (2020). *Managing the Risks of Hydraulic Fracturing*. Fraser.

<https://www.fraserinstitute.org/sites/default/files/managing-the-risks-of-hydraulic-fracturing-2020.pdf>

Myers, T. (2012). Potential Contaminant Pathways from Hydraulically Fractured Shale to Aquifers. *Groundwater*, 50(6), 872–882. <https://doi.org/10.1111/j.1745-6584.2012.00933.x>

Nabizadeh, E., Pepper, D. W., & Waters, J. (2016). *Simulating Hydraulic Fracturing and Contaminant Transport with MATLAB® and COMSOL Multiphysics® Software* [Conference presentation abstract]. COMSOL Conference, Boston, USA. [https://www.comsol.com/paper/download/362241/pepper\\_abstract.pdf](https://www.comsol.com/paper/download/362241/pepper_abstract.pdf)

Nandlal, K., & Weijermars, R. (2019). Drained rock volume around hydraulic fractures in porous media: planar fractures versus fractal networks. *Petroleum Science*, 16(5), 1064–1085. <https://doi.org/10.1007/s12182-019-0333-7>

- Osborn, S. G., Vengosh, A., Warner, N. R., & Jackson, R. B. (2011). Methane contamination of drinking water accompanying gas-well drilling and hydraulic fracturing. *Proceedings of the National Academy of Sciences*, 108(20), 8172–8176. <https://doi.org/10.1073/pnas.1100682108>
- Osselin, F., Nightinglae, M., Hearn, G., Kloppmann, W., Gaucher, E., Clarkson, C.R., & Mayer, B. (2018). Quantifying the extent of flowback of hydraulic fracturing fluids using chemical and isotopic tracer approaches. *Applied Geochemistry*, 93, 20–29. <https://doi:10.1016/j.apgeochem.2018.03.008>
- Pfunt, H., Houben, G., & Himmelsbach, T. (2016). Numerical modeling of fracking fluid migration through fault zones and fractures in the North German Basin. *Hydrogeology Journal*, 24(6), 1343–1358. <https://doi.org/10.1007/s10040-016-1418-7>
- Reagan, M. T., Moridis, G. J., Keen, N. D., & Johnson, J. N. (2015). Numerical simulation of the environmental impact of hydraulic fracturing of tight/shale gas reservoirs on near-surface groundwater: Background, base cases, shallow reservoirs, short-term gas, and water transport. *Water Resources Research*, 51(4), 2543–2573. <https://doi.org/10.1002/2014wr016086>
- Ren, F., Ma, G., Fan, L., Wang, Y., & Zhu, H. (2017). Equivalent discrete fracture networks for modelling fluid flow in highly fractured rock mass. *Engineering Geology*, 229, 21–30. <http://dx.doi.org/10.1016/j.enggeo.2017.09.013>
- Robart, C. J. (2012). *Water Management Economics in the Development and Production of Shale Resources*. International Association for Energy Economics Forum. <https://www.iaee.org/en/publications/newsletterdl.aspx?id=157>

Sarkar, S., Haghihi, M., Sayyafzadeh, M., Cooke, D., Pokalai, K., & Mohamed, F.

(2016). A Cooper Basin simulation study of flow-back after hydraulic fracturing in tight gas wells. *The APPEA Journal*, 56(1), 369-392.

<https://doi.org/10.1071/AJ15027>

Schultz, R., Atkinson, G., Eaton, D.W., Gu, Y.J., & Kao, H. (2018). Hydraulic fracturing volume is associated with induced earthquake productivity in the Duvernay play. *Science*, 359(6373), 304-308.

<https://doi.org/10.1126/science.aao0159>

Seales, M. B., Dilmore, R., Ertekin, T., & Wang, J. Y. (2017). A Numerical Study of Factors Affecting Fracture-Fluid Cleanup and Produced Gas/Water in Marcellus Shale (Part II). *SPE Journal*, 22 (02). <https://doi.org/10.2118/183632-PA>

Shah, S.N., Patel, H., & Pandya, S. (2015, April 19-20). *Motion of Fracturing Fluid and Associated Environmental Impacts* [Paper Presentation]. Conference: NSF sponsored workshop: Reducing the Impact of Hydraulic Shale Fracturing and Natural Gas Drilling on Environments: Development of Green Fracturing Fluids and Sustainable Remediation and Containment Technologies, Arkansas, USA.

<https://www.researchgate.net/publication/323237538>

Shapiro, S.A., & Dinske, C. (2009). Fluid-induced seismicity: Pressure diffusion and hydraulic fracturing. *Geophysical Prospecting*, 57(2), 301-310.

<https://doi.org/10.1111/j.1365-2478.2008.00770.x>

Sheng, M., Chu, R., Peng, Z., Wei, Z., Zeng, X., Wang, Q., & Wang, Y. (2022).

Earthquakes Triggered by Fluid Diffusion and Boosted by Fault Reactivation in

Weiyuan, China Due to Hydraulic Fracturing. *JGR Solid Earth*, 127(5).

<https://doi.org/10.1029/2021JB022963>

Taherdangkoo, R., Tatomir, A., Anighoro, T., & Sauter, M. (2019). Modeling fate and transport of hydraulic fracturing fluid in the presence of abandoned wells. *Journal of Contaminant Hydrology*, 221, 58-68.

<https://doi.org/10.1016/j.jconhyd.2018.12.003>

Taherdangkoo, R., Tatomir, A., Taylor, R., & Sauter, M. (2017). Numerical investigations of upward migration of fracking fluid along a fault zone during and after stimulation. *Energy Procedia*, 125, 126–135.

<https://doi.org/10.1016/j.egypro.2017.08.093>

Tan, Y., Hu, J., Zhang, H., Chen, Y., Qian, J., Wang, Q., Zha, H., Tang, P., & Nie, Z. (2020). Hydraulic Fracturing Induced Seismicity in the Southern Sichuan Basin Due to Fluid Diffusion Inferred From Seismic and Injection Data Analysis.

*Geophysical Research Letters*, 47(4). <https://doi.org/10.1029/2019GL084885>

U.S. Department of Energy, Energy Information Administration, Independent Statistics & Analysis. (2020, August). *Permian*

*Basin*. [https://www.eia.gov/maps/pdf/Permian\\_Wolfcamp\\_Midland\\_EIA\\_report\\_II.pdf](https://www.eia.gov/maps/pdf/Permian_Wolfcamp_Midland_EIA_report_II.pdf)

Veatch, R. W. (1983). Overview of Current Hydraulic Fracturing Design and Treatment Technology - Part 1. *Journal of Petroleum Technology*, 35(4), 677–687.

<https://doi.org/10.2118/10039-PA>

Wang, F., Li, B., Zhang, Y., & Zhang, S. (2017). Coupled Thermo-Hydro-Mechanical-Chemical Modeling of Water Leak-Off Process during Hydraulic Fracturing in

Shale Gas Reservoirs. *Energies*, 10(12), 1960.

<https://doi.org/10.3390/en10121960>

Yang, Y., Jiang, H., Li, M., Yang, S., & Chen, G. (2015). A mathematical model of fracturing fluid leak-off based on dynamic discrete grid system. *Journal of Petroleum Exploration and Production Technology*, 6(3), 343–349.

<https://doi.org/10.1007/s13202-015-0188-4>

Yang, Z., Yehya, A., Iwalewa, T.M., & Rice, J.R. (2021). Effect of Permeability Evolution in Fault Damage Zones on Earthquake Recurrence. *Journal of Geophysical Research: Solid Earth*, 126(9), e2021JB021787.

Yarushina, V. M., Bercovici, D., & Oristaglio, M. L. (2013). Rock deformation models and fluid leak-off in hydraulic fracturing. *Geophysical Journal International*, 194(3), 1514–1526. <https://doi.org/10.1093/gji/ggt199>

Yehya, A., & Rice, J.R. (2020). Influence of Fluid-Assisted Healing on Fault Permeability Structure. *Journal of Geophysical Research: Solid Earth*, 125(10), e2020JB020553.

Yehya, A., Yang, Z., & Rice, J.R. (2018). Effect of fault architecture and permeability evolution on response to fluid injection. *Journal of Geophysical Research: Solid Earth*, 123(11), 9982-9997.

Yongjun, L., Haiyan, W., Baoshan, G., Ping, L., Limei, G., Jiaquan W., & Xinbin, Y. (2018). Reasons for the low flowback rates of fracturing fluids in marine shale. *Natural Gas Industry B*, 5(1), 35-40. <https://doi.org/10.1016/j.ngib.2017.11.006>

- Yu, W., Wu, K., Zuo, L., Tan, X., & Weijermars, R. (2016, August 1-3). Physical Models for Inter-Well Interference in Shale Reservoirs: Relative Impacts of Fracture Hits and Matrix Permeability. *Proceedings of the 4th Unconventional Resources Technology Conference*. Unconventional Resources Technology Conference, San Antonio, Texas, USA. <https://doi.org/10.15530/urtec-2016-2457663>
- Zanganeh, B., Soroush, M., Williams-Kovacs, J.D., & Clarkson, C.R. (2015, October 20-22). *Parameters Affecting Load Recovery and Oil Breakthrough Time after Hydraulic Fracturing in Tight Oil Wells* [Paper Presentation]. SPE/CSUR Unconventional Resources Conference, Calgary, Alberta, Canada.
- Zhou, Q., Dilmore, R., Kleit, A., & Wang, J. Y. (2016). Evaluating Fracture-Fluid Flowback in Marcellus Using Data-Mining Technologies. *SPE Production & Operations*, 31(02), 133–146. <https://doi.org/10.2118/173364-pa>